The Long-term Decline of the U.S. Job Ladder

Aniket Baksy* Daniele Caratelli† Niklas Engbom‡

February 21, 2026

Abstract

We quantify the contribution of changes to the structure of the U.S. labor market to wage stagnation over the past 40 years. Estimating a structural model of wage and employment dynamics on Current Population Survey data yields three main findings. First, upward job mobility has declined by roughly one-half from the 1980s to the 2010s. Second, this decline is not primarily explained by changes to how efficiently the labor market matches open jobs to searching workers, firms' labor demand, or workers' job-acceptance behavior; instead, it reflects a reduction in the efficiency of on-the-job search, which cross-state evidence links to rising employer concentration and the increased use of noncompete agreements. Third, these changes—and the resulting weakening of the U.S. job ladder—account for about one-third of the slowdown in wage growth between the first and second halves of the post–World War II period.

*University of Melbourne: aniket.baksy@unimelb.edu.au
†danicaratelli@gmail.com
‡CEPR, NBER and New York University Stern School of Business: ne466@nyu.edu
We thank our discussants Alex Clymo, Jason Faberman, Kerstin Holzheu, Guillaume Nevo and Laura Pilossoph, as well as Paolo Martellini, Guido Menzio, Giuseppe Moscarini, Richard Rogerson, Venky Venkateswaran, Gianluca Violante and participants at numerous conferences and seminars for helpful comments and feedback.

1 Introduction

Wage growth in the United States has been historically weak since the early 1980s. As shown by Figure 1, real hourly earnings more than doubled between 1940 and 1970. Since 1980, however, wages have risen by only about 20 percent, despite continued productivity growth. Moreover, much of this modest increase reflects a shift in the composition of the workforce toward older, more educated workers, who tend to earn more. Holding demographics fixed at their 1980s levels, real wage growth since the early 1980s is close to zero.

Figure 1: Real Wages in the United States, 1940–2020

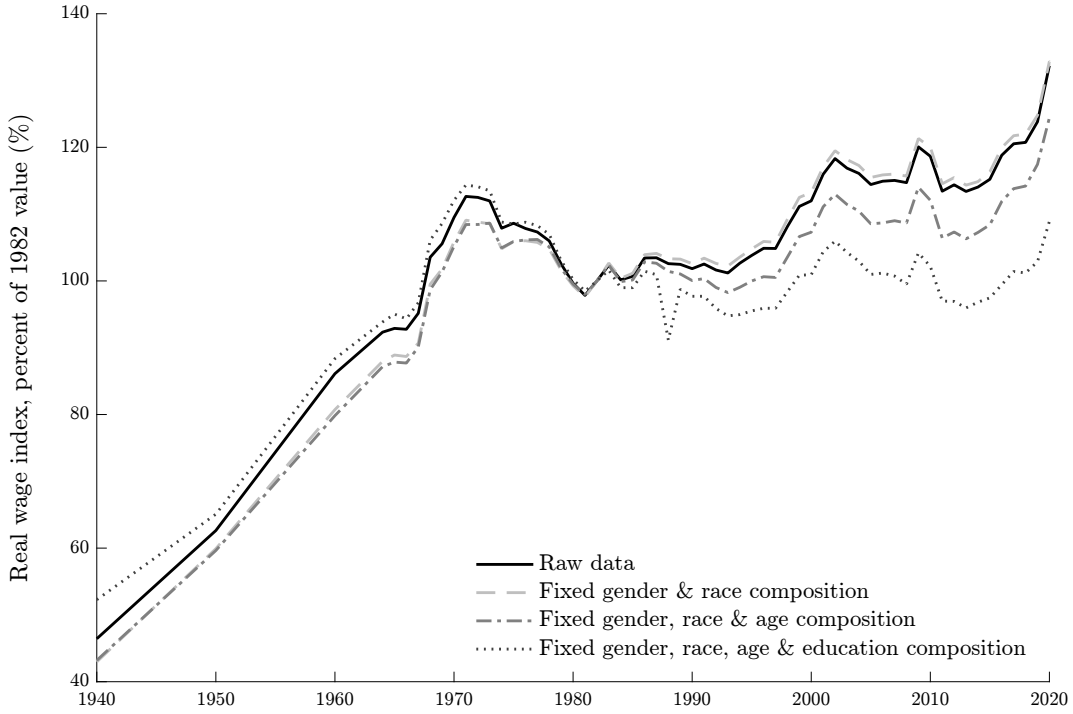

Notes: Hourly wages are constructed as annual labor earnings divided by the product of weeks worked and usual weekly hours (actual hours per week in earlier years). Wages are deflated using the Urban Consumer Price Index (CPI-U). Observations are winsorized at $2.13 in 2022 real hourly wages. "Fixed demographics" reweights the sample to hold constant demographic composition at 1982 levels along various dimensions. The sample includes employees ages 20–59. *Source:* U.S. Decennial Census (1940–1960) and CPS ASEC (1962–2020).

Why did wage growth slow so sharply? A large literature emphasizes skill-biased technical change (Acemoglu, 2002; Autor, 2015), trade exposure (Autor, Dorn and Hanson, 2013), declining unions (Farber et al., 2018), and the falling real value of the federal minimum wage (Lee, 1999; Card and DiNardo, 2002), among other factors. While these forces explain important shifts in the wage structure, they are largely silent on changes to the functioning of the U.S. labor market and their impact on worker reallocation across employers. Motivated by evidence that mobility toward higher-paying employers is a central source of individual earnings growth (Topel and Ward, 1992; Haltiwanger, Hyatt and McEntarfer, 2018), we quantify the contribution of structural

changes in the U.S. labor market and the resulting decline of upward job mobility to wage stagnation over the past 40 years. Our preferred estimate implies that such changes account for a third of the deceleration in wage growth between the first and second halves of the post-WWII period.

Our analysis proceeds in three parts. First, we develop and implement a transparent measure of upward job mobility using a canonical job-ladder model and repeated cross-sectional microdata. Our starting point is a partial-equilibrium model of worker dynamics with on-the-job search and heterogeneous wage offers. Nonemployed workers receive job offers at some rate, with offered wages drawn from an *offer distribution*. Once employed, workers may separate to nonemployment or receive outside offers. Some outside offers are systematically *directed* toward higher-paying jobs, while others are *undirected*, generating job-to-job moves that may involve wage cuts (Jolivet, Postel-Vinay and Robin, 2006). A central implication is that the cross-sectional wage distribution first-order stochastically dominates the offer distribution (Mortensen, 2003). Moreover, the distance between the two distributions—what Christensen et al. (2005) call the *employment effect*—summarizes the intensity of upward job mobility: more frequent directed offers widen the gap by accelerating movement toward higher-paying employers.

Guided by this mapping, we estimate long-run trends in upward job mobility using publicly available microdata from the CPS from January 1982 to March 2023. To that end, we first residualize log hourly wages on rich observables (including detailed occupation controls) flexibly interacted with time. Based on these residual wages, we nonparametrically estimate the wage and offer distributions, equating the latter with the wage distribution of workers who were nonemployment in the previous month. The wage distribution stochastically dominates the offer distribution throughout the sample, as predicted by the theory. However, the gap has narrowed substantially since the early 1980s, indicating falling upward job mobility. Indeed, we estimate that the arrival rate of better paying outside job offers to employed workers has roughly halved between the 1980s and 2010s. The decline has been broad-based across gender, race, and education groups, and has been especially sharp for young workers and new cohorts.

Because the textbook job-ladder model attributes the offer–wage gap entirely to mobility, we also assess robustness to three alternative forces that could affect the gap: wage growth with tenure, selection on unobservables, and recall unemployment/employment-status misclassification (Abowd and Zellner, 1985; Fujita and Moscarini, 2017). Extending the framework to incorporate these features leaves the estimated decline in upward job mobility largely unchanged.

We further confront the predictions of the model with longitudinal data from the 1979 and 1997 National Longitudinal Survey of Youth (NLSY79 and NLSY97). Consistent with the theory, workers experience excess wage growth relative to same-aged peers following a spell of nonemployment, and the bulk of this excess growth is accounted for by subsequent job-to-job mobility. Put another way, to outperform one's peers, job-to-job mobility is central, consistent with the evidence in Ozkan, Song and Karahan (2023). Comparing cohorts, both the frequency of job-to-job moves and the wage gains conditional on moving have declined. The model matches these non-

targeted moments quantitatively well.

In the second part of the paper, we use a general-equilibrium extension to identify the factors responsible for the weakening of the job ladder. To that end, we embed the partial-equilibrium model in general equilibrium through an aggregate matching function (Petrongolo and Pissarides, 2001). In this environment, the job-finding rates of the nonemployed and employed are functions of how efficiently the labor market matches open jobs with searching workers, firms' vacancy creation, and workers' job acceptance behavior. Crucially, the theory highlights that changes in these objects scale the job finding rates from nonemployment and employment proportionally. In the data, however, the former has declined only modestly, while the latter has fallen sharply. This divergence points to a decline in the *efficiency of employed search*.

We then use variation across states over time to investigate potential drivers of employed-search efficiency. Motivated by recent work, we focus on employer concentration (Bagga, 2023) and the prevalence of noncompete agreements (Gottfries and Jarosch, 2023). States with larger increases in concentration and states with higher noncompete prevalence have experienced larger declines in the efficiency of employed search, consistent with these forces making it harder for workers to shop for alternative jobs. Quantitatively, our estimates are in line with or somewhat conservative relative to the estimated impact of concentration on mobility in Berger et al. (2023) as well as that of noncompetes on mobility in Lipsitz and Starr (2022). A back-of-the-envelope calculation using our estimates suggests that these two forces can account for roughly 60 percent of the national decline in employed-search efficiency between the 1980s and 2010s.

In the third part of our analysis, we endogenize the offer distribution following Burdett and Mortensen (1998) in order to quantify the impact of the estimated changes to the structure of the labor market on aggregate wages. Firms that differ in their productivity post wages above workers' reservation wages to recruit and retain workers. While the baseline framework successfully rationalizes the upper part of the offer distribution, it cannot replicate its thin left tail, even under a fully nonparametric productivity distribution (Bontemps, Robin and den Berg, 2000). To match the left tail, we introduce an efficiency gain from higher pay (Shapiro and Stiglitz, 1984).

We start by analyzing theoretically how a decline in the efficiency of employed search affects wages. With less upward job mobility, potential hires are worse matched in the labor market and current employees are less likely to receive better outside offers. For both reasons, firms post lower wages. At the same time, less efficient on-the-job search changes workers' option value of accepting employment, typically (but not necessarily) raising their reservation wage. The rise in the reservation wage puts upward pressure on wages, also higher up the distribution.

We then confront a calibrated version of the model with cross-state variation in the structure of the labor market and wages. To that end, we calibrate the remaining parameters of the model at the national level, and feed into the calibrated economy estimated cross-state differences in the structure of the labor market. Holding fixed underlying firm productivity and the efficiency pay schedule, we assess the impact on aggregate wages. States with greater upward job mobility

have higher wages conditional on observables (including three-digit occupation), which the model matches quantitatively well. Although we might expect higher wages as workers move up the job ladder more, we also show that *offered* wages are higher, consistent with the theoretical prediction that greater employed search efficiency encourages firms to post higher wages.

Finally, we use the model to aggregate to the national time trend. We find that the estimated changes to the structure of the U.S. labor market over the past 40 years and the resulting decline of the U.S. job ladder have reduced the annual growth rate of composition-adjusted real wages by 0.19–0.71 percentage points, with the exact magnitude dependent on the particular assumptions we make about the utility function and how the reservation wage adjusts. The effect is smallest under linear utility and a fixed flow value of nonemployment, in which case the falling efficiency of employed search results in a sharp—but in several regards counterfactual—rise in the reservation wage. Under our preferred specification with log utility and a fixed replacement rate, the growth rate falls by 0.68 percentage points. Given that composition-adjusted real wage growth was just over two percent per year between the 1940s and 1970s and close to zero between the 1980s and 2010s, the weakening of the job ladder accounts for a third of the slowdown in wage growth over this period under our preferred estimate.

Literature. This paper relates to three strands of work. First, it builds on equilibrium models of on-the-job search, wage posting, and frictional wage dispersion (Burdett and Mortensen, 1998; Bontemps, Robin and den Berg, 2000; Postel-Vinay and Robin, 2002), to which Christensen et al. (2005) add endogenous search effort. Most closely related, Jolivet, Postel-Vinay and Robin (2006) use a partial equilibrium search model similar to ours to document differences in upward job mobility across a set of developed countries. Similar to us, they find "that cross-sectional data on individual wages contain the basic information needed to obtain a reliable measure of the 'magnitude of labor market frictions', as measured by a parameter of the canonical job search model." Relative to them, we provide extensions that allow for other potential drivers of the wage-offer gap, and we apply the framework to understand long-run trends in upward job mobility.

A second literature studies job mobility as a driver of wage growth and wage inequality (Topel and Ward, 1992; Haltiwanger, Hyatt and McEntarfer, 2018; Autor, Dube and McGrew, 2023). A complementary empirical literature develops and validates measures of employer-to-employer transitions and documents their secular and cyclical properties (Fallick and Fleischman, 2004; Fujita, Moscarini and Postel-Vinay, 2024). An important insight from our analysis is that trends in the overall job-to-job mobility rate are not necessarily that informative of underlying trends in worker mobility systematically directed toward higher paying jobs. The reason is that a large share of job-to-job transitions are not systematically directed toward higher paying jobs.

Third, a rapidly growing literature quantifies the impact of labor market power on wages, employment, and mobility (e.g., Azar et al., 2020; Prager and Schmitt, 2021; Azar, Marinescu and Steinbaum, 2022; Berger, Herkenhoff and Mongey, 2022; Benmelech, Bergman and Kim, 2022;

Rinz, 2022; Autor, Dube and McGrew, 2023; Caldwell and Danieli, 2024). We relate our evidence on employed-search efficiency to recent work on employer concentration (Bagga, 2023; Berger et al., 2023) and to evidence on the prevalence and effects of noncompete agreements (Starr, Prescott and Bishara, 2021; Lipsitz and Starr, 2022; Gottfries and Jarosch, 2023).

The remainder of the paper is organized as follows. Section 2 introduces the baseline model. Section 3 presents the data and Section 4 our main findings. Section 5 investigates the causes of the decline in upward job mobility, while Section 6 quantifies its implications. Section 7 concludes.

2 A Prototypical Partial Equilibrium Job Ladder Model

Our starting point is a textbook partial-equilibrium random-search model with wage dispersion.

2.1 Setting

Time is continuous and the economy is in steady state.[1] A unit mass of risk-neutral workers move across jobs and between employment and nonemployment. An employed worker's log wage decomposes into observables $\mathbf{X}$, age-based human capital $h(a)$, and a residual firm piece rate w

$$W = \underbrace{\mathbf{X}}_{\text{gender, race, education, state, occupation}} + \underbrace{h(a)}_{\text{human capital via age/experience}} + \underbrace{w}_{\text{residual piece rate offered by the firm}}.$$

The controls in $\mathbf{X}$ absorb, among other factors, labor-demand shifts such as occupation-biased technological change (Acemoglu and Restrepo, 2020). Our object of interest is the residual w.

Nonemployed workers receive a job offer at rate p with an associated draw of a wage w from the offer CDF $F(w)$ and density $f(w)$. For now we take $F(w)$ as given and later endogenize it following Burdett and Mortensen (1998). We assume all offers are accepted; with costly vacancy posting, firms would not optimally advertise wages below a common reservation threshold. We relax this assumption in Section 5.1. Employed workers separate into nonemployment at rate δ.

Let $e(t)$ be the probability of employment at time t given employment at time 0. It satisfies

$$\dot{e}(t) = p\big(1-e(t)\big) - \delta e(t), \quad e(0) = 1 \qquad \Longrightarrow \qquad e(t) = \frac{p}{p+\delta} + \frac{\delta}{p+\delta} e^{-(p+\delta)t}. \tag{1}$$

Similarly, let $n(t)$ be the probability of nonemployment at time t given nonemployment at time 0

$$n(t) = \frac{\delta}{p+\delta} + \frac{p}{p+\delta} e^{-(p+\delta)t}. \tag{2}$$

[1] Allowing the nonemployment rate and wage distribution to vary over time adds time-derivative terms to (3)–(4) and requires two additional moments, $\partial G(w,t)/\partial t$ and $\dot{n}(t)$ (both measurable in the CPS). Relaxing the steady-state assumption barely changes our estimates, so for simplicity we impose steady state throughout.

The stationary employment and nonemployment rates are

$$e(\infty) = \frac{p}{p+\delta}, \qquad n(\infty) = \frac{\delta}{p+\delta}. \tag{3}$$

Employed workers receive two types of outside offers. First, at rate $\lambda^e = \phi^e p$ they contact an open job drawn from $F(w)$ and accept if it pays more than their current job. We refer to these as *directed* offers, since they systematically move workers up the wage ladder. The parameter ϕ^e captures how efficiently the employed search for directed offers (relative to the nonemployed).

Second, at rate $\lambda^f = \phi^f p$ workers contact a randomly drawn open job that they pursue regardless of pay, for example because of nonwage amenities. We call these *undirected* offers. As in Jolivet, Postel-Vinay and Robin (2006), they generate job-to-job moves with wage cuts, which are common in the data. We stress that such moves may still be welfare improving.

Let $G(w)$ be the CDF of wages. Since inflows into jobs paying at most w equal outflows

$$0 = -\underbrace{\Big(\delta + \lambda^f + \lambda^e\big(1-F(w)\big)\Big)(1-n)G(w)}_{\text{outflows from jobs with wage} \le w} + \underbrace{F(w)\big(pn + \lambda^f(1-n)\big)}_{\text{hires into a wage} \le w}. \tag{4}$$

Dividing by $(1-n)$, using (3) to substitute for $pn/(1-n)$, and solving yields

$$G(w) = \frac{F(w)}{1+\kappa\big(1-F(w)\big)}, \tag{5}$$

where the *net upward mobility rate* κ is the number of directed offers a worker on average receives between two "reset" events that set her back in her quest to move up the wage ladder

$$\kappa \equiv \frac{\lambda^e}{\delta + \lambda^f}.$$

A higher net upward mobility rate κ implies a larger gap between where workers start when they are hired from nonemployment, $F(w)$, and where they end up in the long run, $G(w)$.

Let $s(w,t)$ be the share of workers who remain with their initial employer through time t, conditional on initial wage w. It satisfies

$$\dot{s}(w,t) = -(\delta+\lambda^f)(1+\kappa(1-F(w)))s(w,t), \qquad s(w,0) = 1.$$

Solving this ODE and aggregating, the overall share of job stayers after t months is

$$stayer(t) = \int e^{-(\delta+\lambda^f)(1+\kappa(1-F(w)))t} dG(w). \tag{6}$$

2.2 Moment Conditions

The model has four parameters $(\delta, p, \kappa, \lambda^f)$, which we estimate in three steps, and subsequently recover λ^e. Based on (1)–(2), (δ, p) can be expressed as functions of the annual NE and EN rates

$$\delta = -\frac{EN}{NE+EN}\frac{\ln\big(1-(NE+EN)\big)}{12}, \qquad p = -\frac{NE}{NE+EN}\frac{\ln\big(1-(NE+EN)\big)}{12}. \tag{7}$$

We use annual (rather than monthly) transition rates because annual mobility better reflects the experience of the typical worker, as we discuss further below.

Next, we estimate κ from (5). We construct nonparametric estimates of the offer density $f(w)$ and wage density $g(w)$ based on the data in the next section. Given $f(w)$, we choose κ to minimize the distance between the implied wage density and its empirical counterpart[2]

$$\kappa = \underset{\hat{\kappa}\geq 0}{\arg\min} \int \left(\frac{(1+\hat{\kappa})\, f(w)}{\big(1+\hat{\kappa}\big(1-F(w)\big)\big)^2} - g(w) \right)^2 dw. \tag{8}$$

With continuous wage support, (5) provides an infinite set of moments, so κ is overidentified. We exploit this to test the model by computing a pointwise restricted estimate $\kappa^r(w)$

$$\kappa^r(w) = \underset{\hat{\kappa}\geq 0}{\arg\min} \left(\frac{F(w)}{\big(1+\hat{\kappa}\big(1-F(w)\big)\big)} - G(w) \right)^2. \tag{9}$$

If the model is correctly specified, then $\kappa^r(w)$ should be identical across the distribution.

Finally, we recover λ^f and λ^e using the share of job stayers over the prior calendar year and (6), adjusting for imperfect recall. Specifically, some respondents who in contemporaneous surveys report to be nonemployed, later claim in retrospective questions that they remained with the same employer throughout the year. Moreover, the incidence of such misreports rises with the amount of time passed between the spell of nonemployment and the retrospective questions. We model this as imperfect recall: a share $\alpha e^{-\beta m}$ of workers who experience a labor market event in month m that would make them a nonstayer nevertheless later report being a stayer.

The share of workers initially earning wage w who *report* being a stayer becomes

$$s(w) = \underbrace{e^{-12\mu(w)}}_{\text{true job stayers during the year}} + \underbrace{\int_0^{12} \alpha e^{-\beta m}\, \mu(w) e^{-\mu(w)m}\, dm}_{\text{workers who experience an event in month } m \text{ but misreport}},$$

[2] Let $f(w)^{\text{model}}$ denote wages among workers who were nonemployed in the previous month in the model, i.e., the offer distribution as measured in the data. In general, $f(w)^{\text{model}} \neq f(w)$ because workers experience additional labor market events within the month. This time-aggregation bias is tiny under our estimated flow rates, so we ignore it.

where $\mu(w) = (\delta + \lambda^f)(1 + \kappa(1 - F(w)))$. Integrating and averaging over $G(w)$ yields

$$stayer \quad = \quad \int \left(e^{-12(\delta+\lambda^f)(1+\kappa(1-F(w)))} + \nu\, A(w) \left(1 - e^{-12(\delta+\lambda^f)(1+\kappa(1-F(w)))}\right)\right) dG(w), \qquad (10)$$

where ν is the average within-year probability of incorrect recall and the adjustment $A(w)$ reflects the fact that separation events are not evenly spaced over the year

$$\nu \quad \equiv \quad \frac{1}{12}\frac{\alpha}{\beta}\left(1 - e^{-12\beta}\right), \qquad A(w) \quad = \quad \frac{12\beta}{1 - e^{-12\beta}} \frac{\mu(w)}{\beta + \mu(w)} \frac{1 - e^{-12(\beta+\mu(w))}}{1 - e^{-12\mu(w)}}.$$

In practice, $A(w)$ it is very close to one, so in most of analysis we impose $A(w) = 1$ for simplicity. Given (δ, p, κ, ν), we choose λ^f to match the observed stayer share and then recover

$$\lambda^e \quad = \quad \kappa(\delta + \lambda^f).$$

3 Data

Our primary data source is the Current Population Survey (CPS), a rotating panel in which households are interviewed for four consecutive months, out of sample for eight months, and then interviewed for four more. We refer to the first four months as months-in-sample (MIS) 1–4 and the second four months as MIS 5–8.

3.1 Variable Construction and Sample Selection

We link individuals using household and person identifiers, age, sex, and race. Changes in CPS identifiers prevent linking during June–July 1985, September–October 1985, and May–October 1995. Allocation flags became generally available in January 1982, and the Census Bureau altered the recording of weekly earnings beginning in April 2023.[3] We therefore focus on January 1982 through March 2023.

Background characteristics. The BMS records labor force status, job-search activity for those not employed, demographics, and occupation in each survey month, which we refer to as BMS 1–4 and BMS 13–16. There are two main challenges to obtaining a consistent data set. First, changes to the coding of variables over time require harmonization. Second, item nonresponse leads the BLS to impute values, and the prevalence and methods of imputation vary over time.

We topcode age at 75, which is the minimum topcode used over our sample. We recode age to the (hypothetical) age in MIS 1, regardless of whether the respondent actually participated. We re-

[3] In January 2023, the Census Bureau began rounding weekly earnings to enhance confidentiality. These changes apply only to new cohorts entering from January 2023 onward. They first affect reported wages when the January 2023 cohort reaches ORG 4 in April 2023. To avoid a break in the wage series, we end the analysis in March 2023.

strict to individuals aged 20–59 at hypothetical CPS entry to focus on prime working-age workers and to avoid retirement-related transitions. We aggregate race into white and nonwhite, and we standardize race within individuals to nonwhite if it was ever reported. We aggregate education into five categories: less than high school, high school diploma, some college, a bachelor's degree, and postgraduate education.[4] Education is standardized to the highest level ever reported. We use a harmonized three-digit occupation coding aligned with the Census Bureau's 2010 occupation classification. We drop individuals with invalid sex, race, age, or education, and we drop individuals with valid wages but missing occupation.

In each month, we classify labor force status as missing, nonemployed, or employed. Allocated employment status is treated as missing. Because the distinction between unemployment and nonparticipation is often blurred (Clark and Summers, 1979), we collapse them into a single nonemployment category. Weekly earnings are only reported for wage and salary workers, so we treat self-employment spells as missing employment status. The employed category includes private and public wage and salary employees. A hire from nonemployment is defined as an individual who is wage-employed in month t and nonemployed in month $t-1$.

Because attrition is not random, we use survey weights, normalized to the respondent's average weight over their time in sample. Moreover, to avoid a mechanical effect of changes to the demographic composition of the workforce, most of our analysis adjusts the provided survey weights so as to hold the age–gender–race–education composition fixed at its 1982–1991 average.

Appendix A.1 discusses the implications of excluding allocated demographics and standardizing demographic variables, and Table A.6 reports summary statistics for the final sample.

Job stayer status. The ASEC is administered to respondents in sample in March (hence its unofficial "March Supplement" name). It collects retrospective information for the prior calendar year, including weeks worked and the number of employers.[5] Allocated responses are treated as missing. We define a *job stayer* as someone who reports working at least 52 weeks with one employer only.[6] To compute the stayer share in year t, we restrict to respondents who enter the CPS in December of year $t-1$ or January of year t and thus appear in the March CPS. Among those employed in January of year t, we compute the fraction classified as stayers for that year.

Measuring wage dynamics among stayers is complicated by timing. From the ORG, we obtain wage observations 12 months apart, but they do not generally overlap with a calendar year. From the second March Supplement, on the other hand, we know if a worker stayed with their employer

[4] We measure education using educational attainment. Prior to 1992, the CPS reports the highest grade attended and whether it was completed. From 1992 onward, it asks directly for the highest level completed. We construct attainment prior to 1992 by accounting for grade completion.

[5] The March CPS includes several oversamples in some years. We do not attempt to link oversampled households to their ASEC responses and drop them from analyses that use ASEC data (Flood and Pacas, 2017). Oversampled households remain in the BMS in the months in which they are interviewed.

[6] We have also used thresholds of 49–52 weeks with similar results.

during the previous calendar year. To illustrate, an individual entering in December of year $t-1$ we know their wage in March of year t and $t+1$. From the March Supplement, we know whether she stayed with her employer from January through December of year t, but not whether she stayed between January and March of year $t+1$. Even so, wage dynamics among those who stayed with their employer for at least nine of the twelve months provide useful information to identify parameters of the model. We hence replicate this timing in model-generated data.

Wages. In MIS 4 and MIS 8, wage and salary workers answer additional earnings and hours questions. We refer to these ORG interviews as ORG 4 and ORG 16.[7] We restrict attention to wage and salary workers when using ORG data. Earnings are reported before taxes and deductions and include overtime, commissions, and tips. For multiple-job holders, earnings refer to the main job. Hourly workers report an hourly wage, while salaried workers report usual weekly earnings and usual weekly hours on the main job.[8] Weekly earnings are topcoded at thresholds that vary over time,[9] and usual weekly hours are topcoded at 99.

We construct hourly wages as the reported hourly wage for hourly workers and as usual weekly earnings divided by usual weekly hours for salaried workers. We convert wages to December 2022 dollars using the seasonally adjusted monthly CPI for all urban consumers. We multiply topcoded wages by 1.5 and winsorize low real hourly wages at \$2.13, following Autor, Dube and McGrew (2023).

Imputation flags are unavailable from January 1994 to August 1995 and are miscoded between 1989 and 1993. For these years, we infer imputation by comparing edited and unedited values in the source data. Where imputation can be identified, we treat allocated earnings and allocated usual weekly hours as missing. For January 1994 to August 1995, we cannot identify imputed earnings, so we retain all observations.

3.2 Non-parametric Estimates of the Wage and Offer Distribuitons

Since our focus is residual wage dynamics, we residualize wages with respect to observables. Specifically, we project log wages on race, gender, education, state, occupation, and survey-month fixed effects, each flexibly interacted with CPS entry year:

$$\ln wage_{it} = \alpha_{ry} + \alpha_{gy} + \alpha_{ey} + \alpha_{sy} + \alpha_{oy} + \alpha_{my} + \tilde{w}_{it}, \tag{11}$$

[7] Only wage and salary workers are intended to answer ORG earnings questions. There are occasional earnings reports for self-employed workers. To maintain consistency, we treat these as missing.

[8] Starting in 1994, respondents with varying hours do not report usual weekly hours. For these workers, we proxy usual hours with actual hours worked on the main job in the reference week.

[9] Topcoding thresholds are \$999 in 1982–1988, \$1,923 in 1989–1997, and \$2,884.61 from 1998 onward.

In the benchmark, we use three-digit occupations. The time trends below are similar with one-digit occupation controls or with no occupation controls, although levels differ.[10] To limit the influence of extreme observations, we drop individuals whose residual wage in ORG 4 or ORG 16 lies below the 0.5th percentile or above the 99.5th percentile of the residual wage distribution.

Over the life cycle, wages likely grow through both job mobility and general human capital accumulation. Because age is correlated with the job-ladder component, we do not control directly for age in (11). Instead, we deflate $\tilde{w}_{it}$ by the average residual wage of hires from nonemployment of the same age in the same year:

$$w_{it} = \tilde{w}_{it} - \overline{\tilde{w}}_{ya}, \qquad \text{where} \qquad \overline{\tilde{w}}_{ya} = \sum_{t \in y} \sum_{i \in \mathcal{H}_{ta}} s_{it}\, \tilde{w}_{it},$$

where $\mathcal{H}_{ta}$ is the set of respondents of age a who are employed in their ORG month but nonemployed in the preceding month, and s_{it} denotes the sampling weight. This yields residual wages net of human capital, which corresponds to the piece rate w in the model.

Finally, we create an equidistant grid for wages between the minimum and maximum residual wage (after truncating the bottom and top 0.5 percent as noted above). The wage distribution $g(w_i)$ is the overall share of workers with residual wage in bin i. The offer distribution $f(w_i)$ is the share of workers who were nonemployed in the previous month who earn a residual wage in bin i. In the baseline, we use $N = 50$ grid points, but results are not sensitive to this.

3.3 A First Look at the Data Through the Lens of the Model

Before turning to changes in the U.S. job ladder over time, we assess the model's fit in the pooled sample. Table 1 reports parameter estimates and targeted moments. Standard errors come from 1,000 bootstrap resamples of the CPS microdata that preserve the panel structure. We estimate monthly transition rates below conventional values from monthly CPS gross flows. Likely reasons include recall unemployment and employment-status misclassification, which inflate high-frequency transitions (Fujita and Moscarini, 2017; Abowd and Zellner, 1985). In extensions, unobserved heterogeneity also generates rapid churn for some workers alongside long spells for others. Because the baseline model abstracts from such features, we target annual transition rates.

Step 2 yields net upward mobility of $\kappa = 0.82$. Given the offer distribution $f(w)$, this parameter maps into the observed wage distribution $g(w)$. Figure 2a shows a close match in the pooled sample. As an overidentification check, Figure 2b plots the restricted estimate $\kappa^r(w)$ from (9), expressed as deviations from its mean. Although the restriction that $\kappa^r(w)$ is constant is rejected, we view the ability of such a simple model to replicate many features of the data as a success.

According to Step 3, 1.5 percent of employed workers per month receive an undirected outside

[10] We obtain similar results when we instead include fully interacted race–gender–education–year fixed effects, plus state–year, occupation–year, and date fixed effects. Adding industry–year fixed effects to (11) has negligible effects.

Table 1: Model Fit and Parameter Estimates Pooling All Years of Data

Parameter estimates			Targeted moments Data	Model	Data	Model
Step 1. Flows in and out of employment						
δ	p		Annual EN rate		Annual NE rate	
0.008	0.019		0.078	0.078	0.196	0.196
(0.000)	(0.000)		(0.000)	(0.000)	(0.000)	(0.000)
Step 2. Net upward mobility						
κ			Wage distribution			
0.816			See Figure 2			
(0.015)						
Step 3. Undirected and directed mobility (assuming $A(w) = 1$)						
ν	λ^f	λ^e	Misreporting		Stayer share	
0.153	0.015	0.019	See Figure A.6		0.769	0.769
(0.006)	(0.000)	(0.000)			(0.001)	(0.001)
Relaxing the assumption $A(w) = 1$						
	0.016	0.019				
	(0.000)	(0.000)				

Notes: Baseline estimates in Step 3 abstracts from the uneven spacing of separation events during a year to impose $A(w) = 1$ for all w. The final row resports the corresponding estimate with the correct $A(w)$. Standard errors (in parentheses) are bootstrap standard errors based on 1,000 resamples that preserve the CPS panel structure. *Source:* CPS ASEC, BMS and ORG, 1982–2021, and authors' calculations.

Figure 2: Model Fit, Pooling All Years

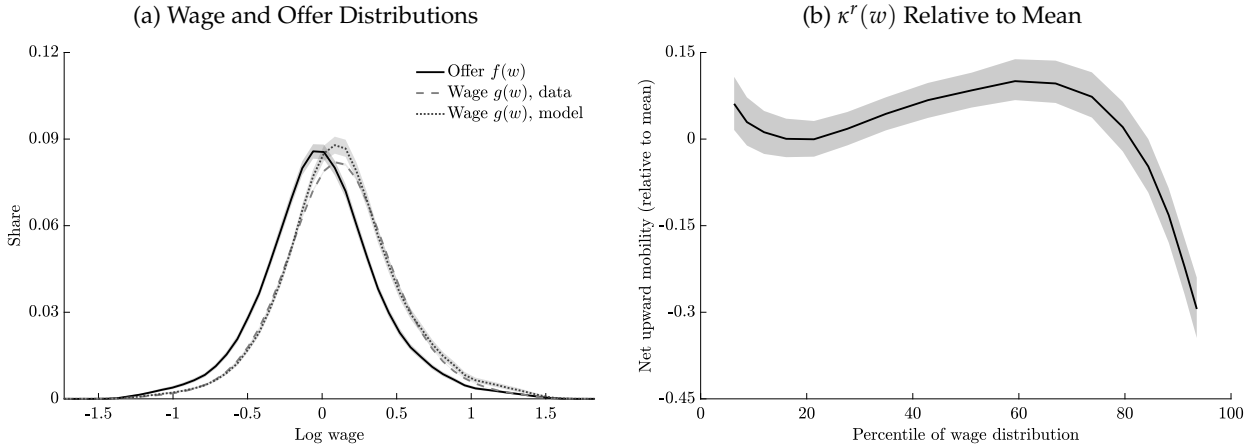

Notes: Panel (a) compares the offer distribution (hires from nonemployment) to the wage distribution in the data and model by decade. Panel (b) plots the restricted estimate $\kappa^r(w)$. Wage construction, trimming, and weighting follow Section 3.1. Shaded areas are bootstrap standard errors based on 1,000 resamples that preserve the CPS panel structure. *Source:* CPS BMS and ORG, 1982–2021, and authors' calculations.

offer that they accept regardless of its wage, while 1.9 percent receive a directed offer that they accept only if it pays more than the current job. Allowing $A(w) \neq 1$ has negligible effects.

4 The Long-Term Decline of the U.S. Job Ladder

We re-estimate the model by decade: 1982–1991, 1992–2001, 2002–2011, and 2012–2021. We then extend the framework and validate its implications using alternative datasets.

Figure 3: Wage and Offer Distributions by Decade

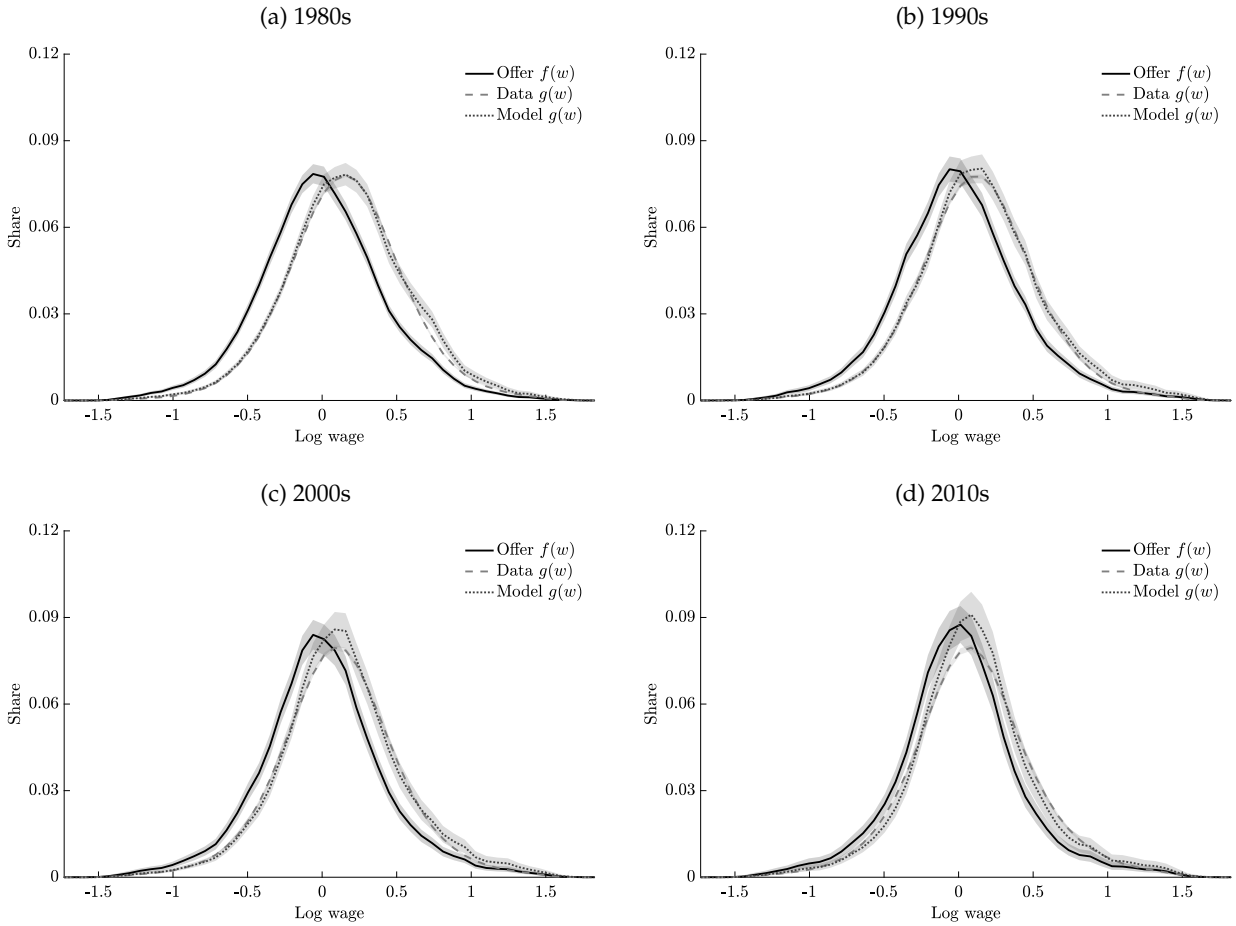

Notes: The offer distribution is the distribution of wages among workers who were nonemployed in the previous month. Residual hourly wages controlling for gender, race, education, 3-digit occupation, state and month all flexibly interacted with year, and deflated by the average residual wage of a hire from nonemployment of the same age in the same year. The provided survey weights are adjusted to keep demographic composition along age-gender-race-education dimensions fixed in the 1980s. Shaded areas are bootstrap standard errors based on 1,000 resamples that preserve the CPS panel structure. *Source:* CPS BMS and ORG, 1982–2021, and authors' calculations.

4.1 Baseline Results

Figure 3 compares the empirical and model-implied wage distributions by decade (the remaining targeted moments are matched exactly in Steps 1 and 3). The model matches the observed wage distribution closely in each decade, with some deterioration of fit over time (our extensions below improve on this). In every decade, the wage distribution first-order stochastically dominates the

offer distribution, but the distance between the two has narrowed over time. Through the lens of a textbook job-ladder model, this narrowing indicates declining net upward job mobility.

Table 2 summarizes our results. We estimate a modest rise in the separation rate δ, a modest fall in the job-finding rate from nonemployment p, a large fall in net upward job mobility κ, and a modest rise in undirected mobility λ^f. Thus, the decline in the net upward job mobility is not compensated for by workers moving more frequently in pursuit of other aspects than higher pay.

Table 2: Parameter Estimates by Decade

	Step 1		Step 2	Step 3		
	δ	p	κ	ν	λ^f	λ^e
1980s	0.007	0.020	1.083	0.097	0.016	0.025
	(0.000)	(0.000)	(0.023)	(0.005)	(0.000)	(0.001)
1990s	0.007	0.020	0.842	0.134	0.016	0.020
	(0.000)	(0.000)	(0.027)	(0.009)	(0.000)	(0.001)
2000s	0.008	0.018	0.753	0.174	0.014	0.016
	(0.000)	(0.000)	(0.030)	(0.013)	(0.000)	(0.001)
2010s	0.008	0.018	0.528	0.216	0.017	0.013
	(0.000)	(0.000)	(0.036)	(0.017)	(0.001)	(0.001)

Notes: Decades correspond to January 1982 to December 1991, January 1992 to December 2001, etc. Standard errors (in parentheses) are bootstrap standard errors based on 1,000 resamples that preserve the CPS panel structure. *Source:* CPS ASEC, BMS and ORG, 1982–2021, and authors' calculations.

In our baseline analysis, we residualize wages using three-digit occupation controls to isolate within-occupation wage dynamics, which we believe the theory is meant to capture. However, trends are similar with one-digit occupation or without occupation controls.

Although changes in demographic composition do not drive our results, since we adjust the survey weights to hold the joint distribution of age, gender, race, and education fixed at its 1980s level, it is of interest to assess whether some groups experienced particularly pronounced changes.

Table 3 reports net upward job mobility κ by decade within demographic group.[11] Women exhibit lower net upward job mobility than men and a larger decline over time, but both groups decline substantially. College graduates are more upwardly mobile than non-graduates, yet mobility roughly halves for both groups. White workers have higher upward job mobility than nonwhite workers, but declines are similar. The decline of the U.S. job ladder is particularly pronounced for young workers/new cohorts. In unreported results, we also find similar declines among dual and

[11] Appendix B.1 shows that for workers with at most $\bar{A}$ time in the labor market,

$$G(w) \quad = \quad \frac{F(w)}{1+\kappa\big(1-F(w)\big)}\,\big(1+C(w;\bar{A})\big), \tag{12}$$

with $C(w;\bar{A}) \to 0$ as $\bar{A} \to \infty$. The adjustment matters mainly for workers with $\lesssim 15$ years of experience. For young-worker estimates we infer (p,δ) from NE/EN rates as before and then jointly estimate (λ^f,λ^e) using (12).

single career households, as well as households with and without children.

Table 3: Net Upward Job Mobility by Subgroup

	Gender		Education		Race		Age	
Decade	Men	Women	No college	College	White	Non-white	Young	All ages
1980s	1.150	1.023	1.026	1.557	1.077	1.099	1.286	1.083
	(0.036)	(0.028)	(0.024)	(0.072)	(0.024)	(0.057)	(0.035)	(0.027)
1990s	0.979	0.739	0.833	1.090	0.872	0.725	0.894	0.842
	(0.040)	(0.034)	(0.029)	(0.062)	(0.029)	(0.057)	(0.037)	(0.031)
2000s	0.811	0.710	0.750	1.018	0.816	0.497	0.768	0.753
	(0.042)	(0.043)	(0.034)	(0.060)	(0.034)	(0.058)	(0.045)	(0.035)
2010s	0.730	0.415	0.521	0.856	0.560	0.423	0.482	0.528
	(0.060)	(0.042)	(0.041)	(0.060)	(0.042)	(0.072)	(0.049)	(0.042)

Notes: "College" denotes workers with a bachelor's degree or higher. "Young" denotes workers aged 20–35; the estimates use the finite-career adjustment in Equation (12). The provided survey weights are adjusted to keep demographic composition along age-gender-race-education dimensions fixed in the 1980s. Sample selection and wage residualization follows Section 3. Standard errors (in parentheses) are bootstrap standard errors based on 1,000 resamples that preserve the CPS panel structure. *Source:* CPS BMS and ORG, 1982–2021, and authors' calculations.

4.2 Robustness

The model interprets the fact that hires from nonemployment earn less than observationally similar workers of the same age as evidence of a job ladder that workers gradually reclimb after a spell of nonemployment.[12] However, similar patterns could arise from wage growth with tenure, mismeasured employment status/recall unemployment, or unobserved heterogeneity. We now extend the model along these dimensions to verify the robustness of our findings.

On-the-job wage dynamics. We model the log wage on the job, $w(t)$, as a mean-reverting process in continuous time with non-Gaussian, thick-tailed shocks. Specifically, while employed

$$dw(t) \;=\; \theta\left(\int w\, f(w)\, dw + \mu - w(t)\right)\, dt \;+\; dJ(t),$$

where $\theta > 0$ governs the speed of mean reversion, μ captures how much wages are expected to grow relative to their level at entry from nonemployment, and $J(t)$ is a symmetric pure-jump Lévy process (a compound Poisson process) that allows for occasional large wage changes on-the-job

$$J(t) \;=\; \sum_{n=1}^{N(t)} Y_n, \qquad N(t) \sim \text{Poisson}(\Lambda t),$$

where the jump sizes $\{Y_n\}$ are i.i.d., symmetric around zero, and have a Pareto-type tail.

[12] Similar results hold if we instead deflate wages by those of similarly experienced workers.

A convenient continuous-time specification is to characterize $J(t)$ by its Lévy measure

$$\nu(dy) \quad = \quad \sigma \frac{1}{|y|^{1+\zeta}} \mathbf{1}\{y_{\min} \leq |y| \leq y_{\max}\}\, dy,$$

so that $\sigma > 0$ scales the overall intensity of jump risk and $\zeta > 0$ controls tail thickness (smaller ζ implies heavier tails, i.e. larger jumps). The total jump arrival rate is $\Lambda = \int \nu(dy)$ and, conditional on a jump, the jump-size density is proportional to $|y|^{-(1+\zeta)}$ on $[y_{\min}, y_{\max}]$.

Employment status misclassification/recall unemployment. A long literature argues that gross flows in the CPS are substantially inflated by employment status misclassification (Abowd and Zellner, 1985). Motivated by these observations, we assume that a fraction ε of employed workers misreport their status as nonemployed at the time they are surveyed. This could alternatively be re-interpreted as recall unemployment—a worker's latent state is employment, but she happens to be temporarily not at work at the time of the survey (Fujita and Moscarini, 2017). Since truly nonemployed workers find jobs at rate p drawn from the true offer distribution $f(w)$, while a share ε of employed workers distributed according to $g(w)$ are recorded as hires from nonemployment in the next month at their previous wage, the observed offer distribution $\widehat{f}(w)$ is

$$\widehat{f}(w) \quad = \quad \frac{npf(w) + (1-n)\varepsilon g(w)}{np + (1-n)\varepsilon}. \tag{13}$$

Hence, employment status misclassification/recall unemployment affects the mapping between the observed and true offer distributions. In particular, if over time a larger share of those we classify as hires from nonemployment are actually recalls to the previous employer at the previous wage, the observed wage and offer distributions will converge ($d(\widehat{F}(w) - G(w))/d\epsilon < 0$).

Permanent unobservable heterogeneity. Figure 4a plots the distribution of respondents over total months in nonemployment during the eight-month CPS panel. A large share of workers spend their entire eight months employed, suggesting a low separation rate. To be consistent with the overall fraction of nonemployed, this also requires a low job-finding rate. However, a fair number of workers are nonemployed for some but not all months, which is inconsistent with low job separation and finding rates. More broadly, the joint distribution of respondents over employment status during the eight-month CPS panel is difficult to reconcile with a homogeneous-worker model with geometric (memoryless) hazards.[13]

Figure 4b plots the average residual wage in ORG 16 as a function of the residual wage in ORG 4 among workers who were nonemployed in at least one of BMS 13–15. According to the textbook job ladder, this relationship should be flat, since a job loss resets the wage.[14] The data, on the other

[13] Although employment status misclassification/recall unemployment generates more short spells of nonemployment, it is not sufficiently strong to match the observed patterns.

[14] Employment status misclassification/recall unemployment implies an upward-sloping relationship, since some

Figure 4: Evidence of Unobserved Heterogeneity

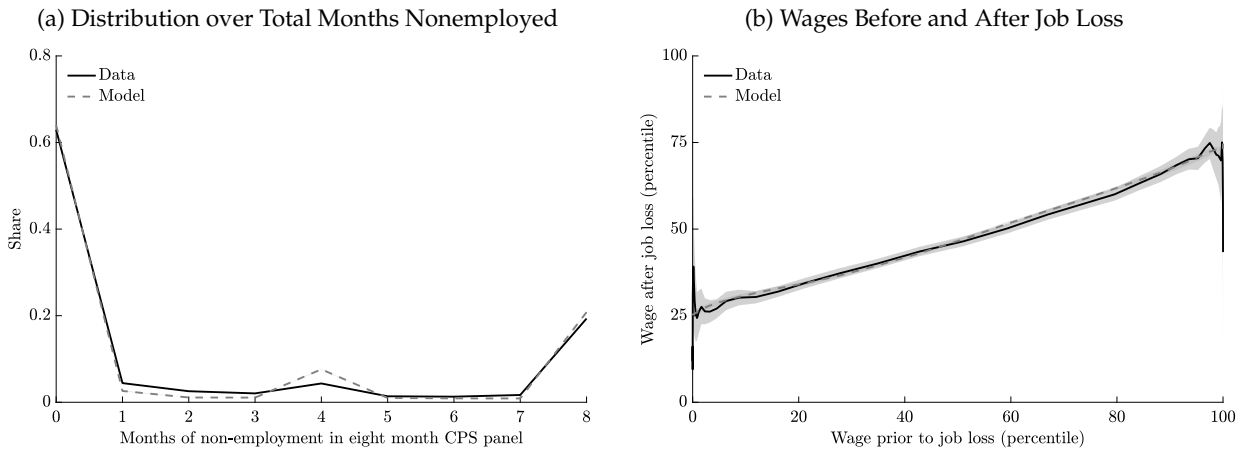

Notes: Panel (a) plots the distribution of total months spent nonemployed during the eight-month CPS panel. Panel (b) plots mean residual wages in ORG 16 against mean residual wages in ORG 4 for workers recorded as nonemployed in at least one of BMS months 13–15. Sample selection and wage residualization follows Section 3. Shaded areas are bootstrap standard errors based on 1,000 resamples that preserve the CPS panel structure. *Source:* CPS BMS and ORG, 1982–2021, and authors' calculations.

hand, indicate that someone who earned more prior to a job loss tends to earn more in their next job (conditional on observables including 3-digit occupation).

Motivated by the patterns in Figure 4, we assume that there are two permanent worker types, $k \in \{1,2\}$,[15] who differ in their separation rate δ^k, where π is the population share of the first type, as well as their offer distributions $f^k(w)$. We label type 2 as "high" and assume that this type samples (log) wages from a normal distribution with mean $\overline{w}^f + \omega$ and standard deviation σ^f, where $\overline{w}^f$ is the mean of the aggregate true offer distribution f and σ^f its standard deviation. The offer distribution of the low type is given residually by

$$f(w) \quad = \quad \frac{n^1}{n} f^1(w) + \frac{n^2}{n} f^2(w), \tag{14}$$

where n^k is the number of nonemployed of type k and $n = n^1 + n^2$ the total nonemployment rate.

Estimation. The extended model features 12 parameters to estimate internally:[16]

$$\mathbf{x} \quad = \quad \left[\, p \, , \, \delta^1 \, , \, \delta^2 \, , \, \pi \, , \, \kappa \, , \, \lambda^f \, , \, \mu \, , \, \theta \, , \, \sigma \, , \, \zeta \, , \, \omega \, , \, \varepsilon \, \right].$$

workers who are recorded as job losers return to their previous job at their previous wage. Yet on its own, this force is not sufficiently strong to fully account for this pattern.

[15] We have tried three unobserved types, but we struggled to identify the third type well using the available data and it did not substantively change the results reported below.

[16] We additionally introduce nonresponse by assuming that a worker drops out of the survey at rate *out* and reenters at rate *in*. Labor market dynamics are identical for respondents who fail to respond. We calibrate the in- and outflow parameters in a first stage to match the fraction of observations with missing employment status in month m that report a nonmissing status in month $m+1$ and vice versa. We also set imperfect recall of stayer status ν as previously.

We estimate these parameters using Simulated Method of Moments. Specifically, for a given set of potential parameter values and the observed offer and wage distributions, we first recover the true aggregate offer distribution from (13). Figure 5a illustrates our inferred true offer distribution, which is shifted to the left of the observed distribution as some respondents who are recorded as a hire from nonemployment in fact return to their previous employer, either due to employment status misclassification or recall unemployment. Subsequently, again under some given parameter values, we recover the type-specific offer distributions from (14). Figure 5b plots the offer distributions of the two types. We feed these type-specific offer distributions into the model to find parameter values to match as well as a set of targets that we discuss further below.

Figure 5: Offer Distribution, Extended Model

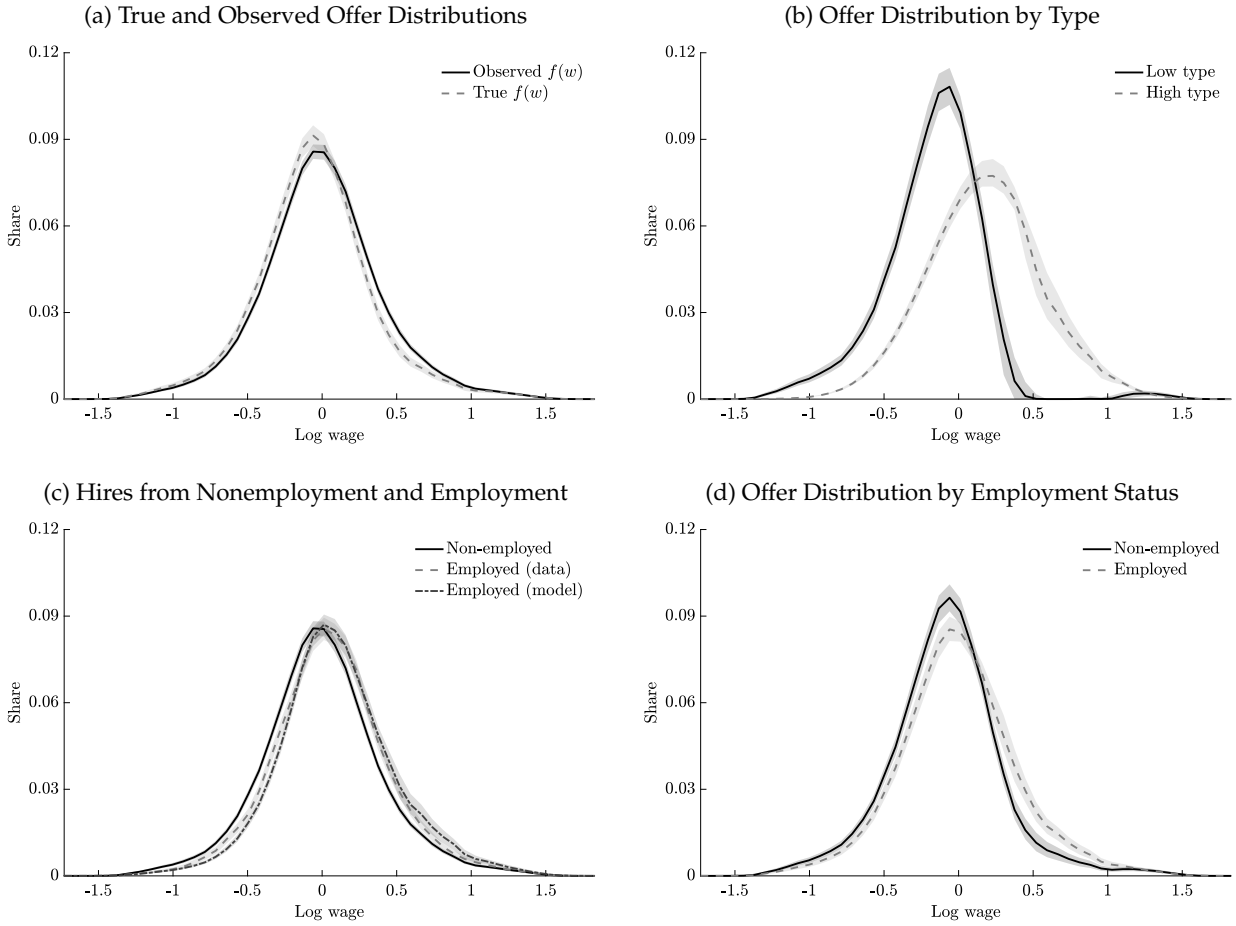

Notes: Panel (a) plots the observed offer distribution constructed from recorded hires from nonemployment and the model-implied offer distribution after adjusting for employment-status misclassification/recall unemployment as in (13). Panel (b) plots the estimated offer distributions for the two unobserved worker types. Panel (c) plots the distribution of wages of hires from nonemployment and from employment in the data and in the model. Panel (d) plots the model-implied offer distributions conditional on employment status. Sample selection and wage residualization follows Section 3. Shaded areas are bootstrap standard errors based on 1,000 resamples that preserve the CPS panel structure. *Source:* CPS ASEC, BMS and ORG, 1982–2021, and authors' calculations.

One important assumption that we maintain throughout is that the nonemployed and em-

ployed face the same offer distribution. Although we cannot directly observe sampled wages of the employed in the CPS, since 1994 we can measure the initial wages of job-to-job switchers, which we can confront with the same outcome in the model. Figure 5c shows that the model matches well the observed distribution of initial wages of hires from employment.

Although we assume that employment status has no causal effect on the offer distribution, selection on unobservables implies that the employed appear to sample better offers. In particular, high-type workers who sample better offers are overrepresented in the pool of employed, so that the average employed worker samples better offers than the average nonemployed worker, as shown in Figure 5d. This pattern is consistent with evidence in Faberman et al. (2022).

Figure 6 plots some of the key additional targets that inform the parameters of the extended model (see Appendix B.2 for a full list of targets). For instance, the model matches well the declining separation rate with the initial wage due to unobserved types with a high separation rate being concentrated at low wages (panel (a)), as well as the share of job stayers by the initial wage (panel (b)). In contrast, a model with only directed mobility would generate a stayer share that rises much too steeply with the initial wage. The extended model further improves on the stylized model's fit of the empirical wage distribution (panel (c)). Finally, it matches well year-on-year wage changes of job stayers, job losers and all workers (panel (d)).

Results. Table 4 reports parameter estimates by decade (Appendix B.2 shows that the extended model fits very well the observed wage distribution in each decade). Accounting for employment status misclassification/recall unemployment increases the inferred gap between true offers and observed wages, which raises estimated net upward job mobility relative to the baseline model. Across decades, we continue to find small movements in p and the separation rates (δ^1, δ^2), a pronounced decline in net upward job mobility κ, and a modest rise in undirected offers λ^f. Net upward job mobility partially rebounds in the last decade, but remains below its 1980s level.

Since 1994, the CPS allows us to construct an aggregate job-to-job transition rate (adjusted as in Fujita, Moscarini and Postel-Vinay (2024)). Figure 7a plots this series and the model counterpart. Although the model is estimated on different moments, it matches both the level and the modest decline in job-to-job mobility well. The model reconciles this modest decline with a large fall in net upward job mobility because (i) many realized transitions are undirected, (ii) undirected mobility rises modestly, and (iii) as directed offers become rarer, acceptance rates rise as workers become more poorly matched.

The rest of Figure 7 provides corroborating evidence of the decline of the U.S. job ladder. Job losers experience smaller wage losses in recent decades (Figure 7b), consistent with a flatter ladder. The share of job stayers rises over time (Figure 7c). In principle, this could be due to a fall in δ, κ or λ^f. The lack of a trend in the EN rate suggests that it is not δ (Figure 7d). Moreover, the particularly large increase at the bottom of the wage distribution is consistent with a fall in κ, whereas a fall in λ^f would lead to a similarly large increase across the distribution.

Figure 6: Model Outcomes in the Extended Model Pooling All Years of Data

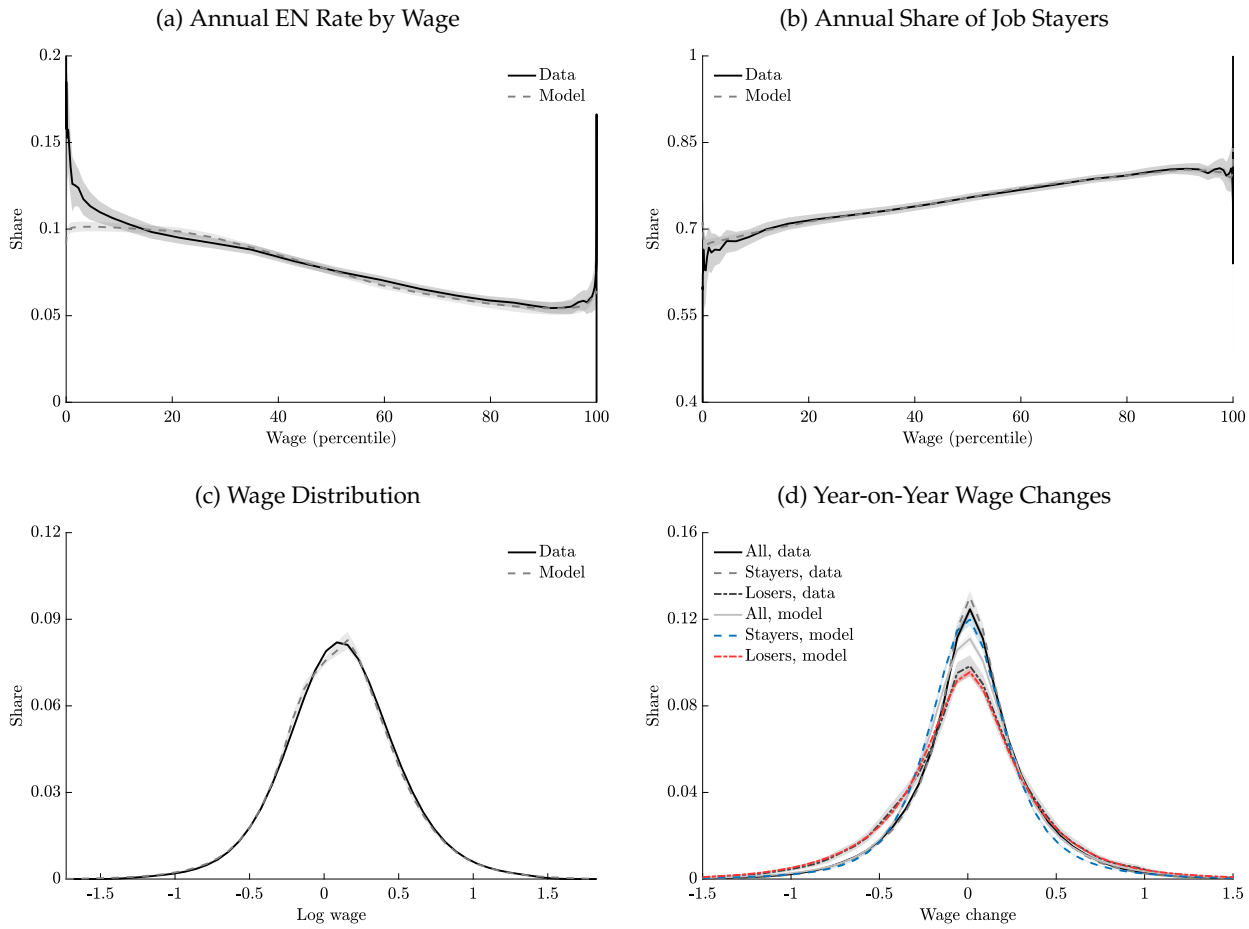

Notes: Panel (a) plots the share of workers who are nonemployed in month $t + 12$ by their percentile of the residual wage distribution in month t. Panel (b) plots the share of workers who remain with the same employer during the previous calendar year—i.e. had only one employer and worked 52 weeks or more—by their percentile in the residual wage distribution in their first ORG month. Panel (d) plots the distribution of year-on-year changes in their residual wage among job stayers, job losers and all workers. Job stayers are those who remained with the same employer during the previous calendar year—this sample is restricted to those in the March supplement. Job losers are those who were non-employed in at least one of BMS 13-15. Model moments are constructed identically to the data. Sample selection and wage residualization follows Section 3. Shaded areas are bootstrap standard errors based on 1,000 resamples that preserve the CPS panel structure. *Source:* CPS ASEC, BMS and ORG, 1982–2021, and authors' calculations.

4.3 Direct Evidence of a Decline in Upward Job Mobility

Our analysis so far infers a decline in upward job mobility from the model and primarily cross-sectional wage data. We now test these implications using longitudinal wage and employment dynamics in the NLSY. Specifically, we use the NLSY79 and NLSY97 cohorts, which entered the U.S. labor market in the early 1980s and early 2000s. We restrict to 1978–2022 and workers aged 22–38 after completing schooling, and reweight observations so the age-gender-race-education composition in the 1997 survey matches that in 1979. We convert hourly wages to real terms, winsorize at \$2.13 (2022 dollars), remove person fixed effects, deflate residual wages by the mean

Table 4: Parameter Estimates by Decade in Extended Model

Parameter	Explanation	1980s	1990s	2000s	2010s
p	Job finding rate of nonemployed	0.019	0.021	0.018	0.018
		(0.000)	(0.000)	(0.000)	(0.001)
δ^1	Separation rate of low type	0.013	0.011	0.014	0.015
		(0.001)	(0.001)	(0.002)	(0.006)
δ^2	Separation rate of high type	0.004	0.004	0.004	0.004
		(0.000)	(0.000)	(0.001)	(0.001)
π	Share of low type	0.410	0.425	0.424	0.433
		(0.034)	(0.051)	(0.066)	(0.117)
κ	Net upward mobility rate	1.651	1.300	0.518	0.899
		(0.176)	(0.208)	(0.147)	(0.197)
λ^f	Undirected mobility rate	0.012	0.014	0.016	0.014
		(0.001)	(0.001)	(0.001)	(0.002)
μ	Wage growth on-the-job	0.012	0.011	0.004	-0.046
		(0.030)	(0.026)	(0.025)	(0.034)
θ	Autocorrelation of wages on the-job	0.028	0.037	0.041	0.039
		(0.001)	(0.002)	(0.003)	(0.003)
σ	Frequency of wage shocks	0.114	0.121	0.166	0.126
		(0.011)	(0.018)	(0.034)	(0.031)
ζ	Shape of wage shocks	1.734	1.560	1.743	1.458
		(0.076)	(0.101)	(0.166)	(0.166)
ω	Mean difference in offer distributions	0.307	0.304	0.293	0.275
		(0.013)	(0.016)	(0.019)	(0.034)
ϵ	Employment status misclassification	0.003	0.003	0.002	0.003
		(0.000)	(0.000)	(0.000)	(0.001)

Notes: Decades refer to January 1982 to December 1991, etc. The provided survey weights are adjusted to keep demographic composition along age-gender-race-education dimensions fixed in the 1980s. Parameters are estimated by simulated method of moments targeting 14,427 moments. Sample selection and wage residualization follows Section 3. Standard errors (in parentheses) are bootstrap standard errors based on 1,000 resamples that preserve the CPS panel structure. *Source:* CPS ASEC, BMS and ORG, 1982–2021, and authors' calculations.

residual wage of same-age hires from nonemployment, and bin wages onto the model wage grid.

We identify spells that begin with a hire from nonemployment and track respondents for up to 120 months, allowing for subsequent nonemployment and reemployment. When a respondent experiences multiple such spells, we treat each spell separately. We compute wage profiles and event rates as a function of months since the hire and replicate these objects in the model.

Figure 8 plots residual wage growth following a hire from nonemployment, relative to same-age peers. For the earlier cohort, excess wage growth over the first 10 years is about 13 log points; it is smaller for the later cohort. The model matches both profiles closely, though it slightly understates the decline in excess wage growth across cohorts.

Figure 7: Supporting Evidence from the CPS

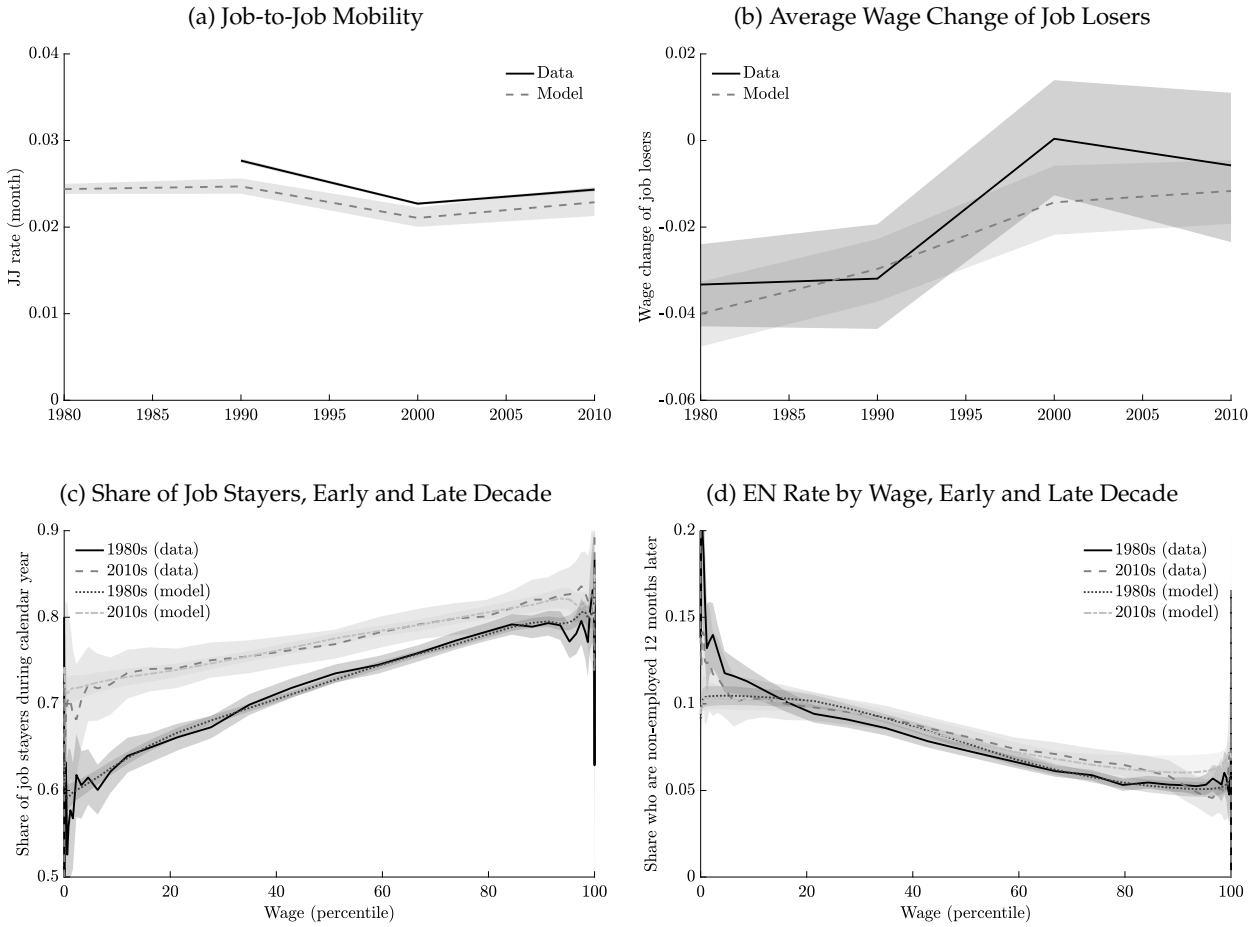

Notes: Panel (a) plots the aggregate job-to-job mobility rate; the data series is adjusted following Fujita, Moscarini and Postel-Vinay, 2024. Panel (b) plots the average year-on-year change in residual wages among workers who were nonemployed in at least one of BMS 13-15. Panels (c) plots the share of workers who remained with the same employer during the previous calendar year by their percentile of the residual wage distribution in their first ORG month. Panel (d) plot the share of workers who are nonemployed in month $t+12$ by their percentile of the residual wage distribution in month t. Wage residualization and sample follow Section 3. Shaded areas are bootstrap standard errors based on 1,000 resamples that preserve the CPS panel structure. *Source:* CPS ASEC, BMS and ORG, 1982–2021, and authors' calculations.

In principle, excess wage growth after nonemployment could reflect within-employer progression (e.g., returns to tenure) or gains associated with job-to-job transitions. Table 5 shows that, in both the data and the model, mover gains account for most of the excess growth: stayer wage changes are near zero, whereas movers experience sizable gains. Both the mover share and the conditional gain from moving decline across cohorts.[17] The model attributes this shift to a higher share of undirected moves, which are on average associated with wage losses.

[17]The definition of the job-to-job transition rate in Table 5 differs slightly from that in Figure 7a: the former is the share of workers employed in either month t or $t+1$ who are at different employers in t and $t+1$, whereas the latter conditions on being employed in month $t+1$.

Figure 8: Wage Growth After a Spell of Nonemployment

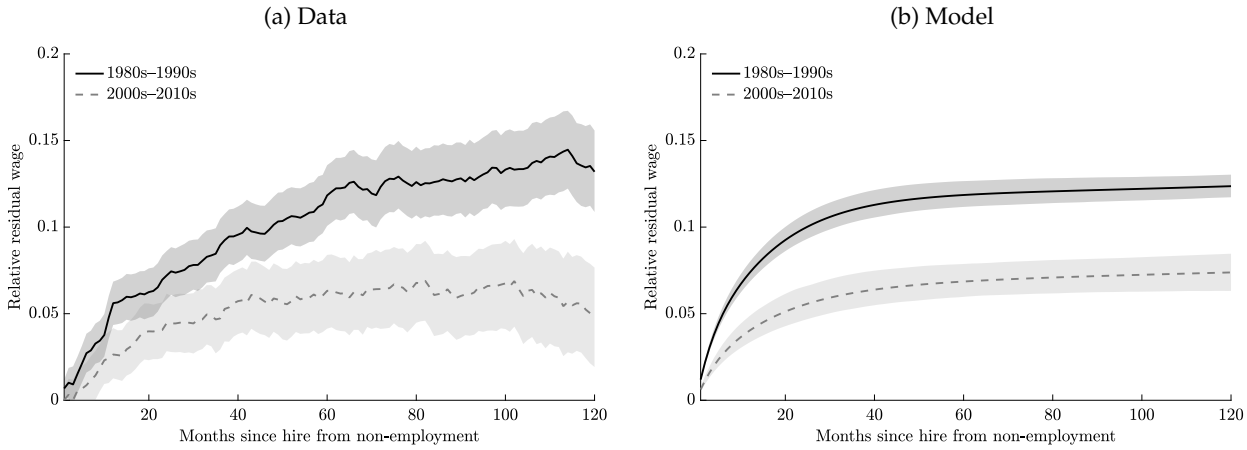

Notes: Figure 8 plots the average residual log wage of workers who are hired from nonemployment in month $t = 0$, separately for the 1979 and 1997 cohorts. Wages in the data are residualized by removing person fixed effects, deflated by the average residual wage of same-age hires from nonemployment, and expressed relative to the wage at time $t = 0$. The sample is restricted to workers aged 22–38 who have completed their highest degree. The provided survey weights are adjusted to hold demographic composition along age-gender-race-education fixed at the earlier cohort. The early cohort in the model is the average across the 1980s-1990s cohorts and the late cohort is the average across the 2000s-2010s cohorts. Shaded areas are bootstrap standard errors based on 1,000 resamples that preserve the CPS/NLSY panel structure. *Source:* NLSY 1979 and 1997 and CPS ASEC, BMS and ORG, 1982–2021, and authors' calculations.

5 The Causes of the Decline of the U.S. Job Ladder

Our partial equilibrium analysis uncovers a large decline in upward job mobility in the U.S. over the past 40 years, but it is silent on its causes. This section analyzes what caused the decline.

5.1 Declining Search Efficiency On-the-Job

Benchmark equilibrium models point to several mechanisms that can reduce upward job mobility, including lower aggregate matching efficiency, weaker labor demand, and changes to workers' acceptance behavior. To analyze the role of these factors, suppose the offer-arrival rate, $\widehat{p}$, depends on vacancies V, searchers S, and matching efficiency χ through an aggregate matching function

$$\widehat{p} \;=\; \chi \left(\frac{V}{S}\right)^{\alpha}. \tag{15}$$

Suppose furthermore that nonemployed workers accept only offers paying at least r. Appendix C.1 shows that the job-finding rate is the product of the offer-arrival rate and the acceptance rate

$$\underbrace{p}_{\text{job-finding rate}} \;\equiv\; \underbrace{\widehat{p}}_{\text{offer-arrival rate}} \times \underbrace{\left(1-\widehat{F}(r)\right)}_{\text{acceptance rate}}, \tag{16}$$

Table 5: NLSY Wage Outcomes: Model vs. Data

	1980s–1990s		2000s–2010s		Change	
	Model	Data	Model	Data	Model	Data
$\overline{w}_{120} - \overline{w}_1$	0.074	0.109	0.047	0.048	-0.027	-0.061
	(0.002)	(0.010)	(0.004)	(0.012)	(0.005)	(0.016)
$\overline{\Delta w^{\text{stayer}}}$	-0.002	-0.000	-0.002	-0.001	0.000	-0.000
	(0.000)	(0.000)	(0.001)	(0.000)	(0.001)	(0.000)
$\overline{\Delta w^{\text{mover}}}$	0.135	0.099	0.108	0.081	-0.027	-0.018
	(0.015)	(0.005)	(0.020)	(0.009)	(0.024)	(0.011)
Share movers	0.020	0.022	0.019	0.018	-0.001	-0.004
	(0.000)	(0.000)	(0.001)	(0.000)	(0.001)	(0.001)

Notes: $\overline{w}_{120} - \overline{w}_1$ is cumulative residual wage growth from months 1-12 to months 97–120 after a spell of nonemployment. $\overline{\Delta w^{\text{stayer}}}$ and $\overline{\Delta w^{\text{mover}}}$ are mean monthly residual wage changes for job stayers and job movers, respectively. "Share movers" is the fraction of workers employed in either month t or $t+1$ who report a different employer between t and $t+1$. Wages in the data are residualized by removing person fixed effects, deflated by the average residual wage of same-age hires from nonemployment, and expressed relative to the wage at time $t = 0$. The sample is restricted to workers aged 22–38 who have completed their highest degree. The provided survey weights are adjusted to hold demographic composition along age-gender-race-education fixed at the earlier cohort. The early cohort in the model is the average across the 1980s-1990s cohorts and the late cohort is the average across the 2000s-2010s cohorts. Standard errors (in parentheses) are bootstrap standard errors based on 1,000 resamples that preserve the CPS/NLSY panel structure. *Source:* NLSY 1979 and 1997 and CPS ASEC, BMS and ORG, 1982–2021, and authors' calculations.

where $\widehat{F}$ is the (unobserved) untruncated offer distribution. Similarly, the arrival rate of acceptable directed outside offers to employed workers is

$$\lambda^e \equiv \underbrace{\phi^e}_{\text{on-the-job search efficiency}} \times \underbrace{\widehat{p}}_{\text{offer-arrival rate}} \times \underbrace{\left(1 - \widehat{F}(r)\right)}_{\text{acceptance rate}}. \tag{17}$$

Our estimation identifies the realized rates p and λ^e, not the underlying arrival rates $\widehat{p}$ and $\phi^e\widehat{p}$.

Equations (15)–(17) imply that changes in matching efficiency (χ), firms' vacancy creation decisions (V), and workers' search behavior (S, r and $\widehat{F}$) move the job offer arrival rate of the nonemployed and employed proportionally. Our estimates, on the other hand, indicate only a modest decline in p but a large drop in λ^e, pointing to a decline in on-the-job search efficiency ϕ^e.

5.2 Factors Behind the Decline in Employed Search Efficiency

Two mechanisms that could reduce the efficiency of on-the-job search are rising employer concentration (Bagga, 2023; Berger et al., 2023) and the growing use of non-compete agreements (Lipsitz and Starr, 2022; Gottfries and Jarosch, 2023). Higher concentration limits opportunities for job shopping, while non-competes directly restrict mobility of the employed. We provide new evidence on the impact of these forces based on variation across U.S. states over time.

We first obtain $(\delta_{sd}, p_{sd}, \lambda^f_{sd}, \kappa_{sd})$ for each state s and decade d from the baseline model estimated separately by state-decade.[18] We merge these estimates with state-decade measures of employer concentration from the Census Bureau's *Business Dynamics Statistics* (BDS) and with state-level non-compete prevalence in 2022–2024 from the *Survey of Household Economics and Decisionmaking* (SHED). Let $\Delta x \equiv x_{s,2010} - z_{s,1980}$ denote the change in one of $x = \{\kappa, \lambda^e, p, \phi^e\}$ between the 1980s and 2010s in state s and $\Delta concentration_s$ the corresponding change in either the employment share of establishments with 100+ employees or log average establishment size. We project the change in outcome x on the change in concentration and the prevalence of non-competes

$$\Delta\phi^e_s \quad = \quad \beta_0 + \beta_1 \Delta concentration_s + \beta_2 noncompete_s + \varepsilon_s.$$

Unfortunately, historical time series on non-compete agreements are unavailable, so we use contemporaneous non-compete prevalence as a proxy for the change in their use and enforcement between the 1980s and 2010s. We motivate this proxy with the view of legal experts that "decades ago, non-compete agreements were widely regarded with suspicion and limited to only a handful of high-ranking employees within a given company. That began changing in the 1980s and picked up steam over the next couple decades. The era from 1990 through circa 2010 was the Golden Age of non-compete enforcement in America. Big firm corporate lawyers built entire practices dedicated to non-compete enforcement."[19] To the extent that contemporaneous prevalence is an noisy proxy for the change, we would expect any estimated relationships to be attenuated.

Table 6 shows that states with larger increases in concentration—and states with higher non-compete prevalence—experienced larger declines in net upward mobility, κ. This relationship operates entirely through the arrival rate of directed outside offers, λ^e, with little association with separations δ or the arrival rate of undirected offers λ^f. Moreover, the decline in $\lambda^e = \phi^e p$ reflects changes in employed-search efficiency, ϕ^e, rather than changes in the job-finding rate per unit of search efficiency, p. Panel specifications with state and decade fixed effects yield similar patterns for the concentration measures (data limitations prevent running analogous panels for non-competes). Overall, the evidence is consistent with concentration and non-competes lowering the effectiveness of on-the-job search by reducing scope for job shopping.

In terms of magnitudes, the estimates in Panel A imply that a one percentage point increase in the employment share of establishments with 100+ employees is associated with a 0.061 percentage point decline in the monthly arrival rate of directed outside offers, λ^e. The unweighted cross-sectional standard deviation of the change in the employment share of 100+ establishments is 3.7 percentage points. Hence, a one standard deviation larger increase in the employment share of 100+ establishments is associated with a $0.061 \times 0.037 \approx 0.23$ percentage point larger decline in

[18] To increase sample size for our nonparametric estimate of the offer distribution, we proxy the offer distribution using residual wages among workers who report being nonemployed at some point in the previous three months.

[19] Pollard PLLC, "Franchise Non-Compete Agreements: Mostly Unenforceable as Written," July 6, 2018, https://pollardllc.com/franchise-non-compete-agreements/ (accessed February 19, 2026).

Table 6: Cross-State Evidence on Employer Concentration and Non-Compete Agreements

	κ	λ^e	p	ϕ^e
Panel A. Employment share of 100+ establishments, 1980–2010 change				
Employment share of 100+ estab.	-2.207**	-0.061***	0.017***	-3.031***
	(1.073)	(0.023)	(0.006)	(1.170)
Share of workers with non-compete	-1.776*	-0.032	0.007	-1.809*
	(0.976)	(0.021)	(0.006)	(1.064)
Panel B. Log average establishment size, 1980–2010 change				
Log average establishment size	-0.814*	-0.022**	0.005*	-1.200**
	(0.484)	(0.010)	(0.003)	(0.528)
Share of workers with non-compete	-1.787*	-0.032	0.007	-1.830*
	(0.990)	(0.021)	(0.006)	(1.081)
Panel C. Employment share of 100+ establishments, state-decade panel				
Employment share of 100+ estab.	-1.908**	-0.055***	0.015**	-2.817***
	(0.907)	(0.020)	(0.007)	(0.967)
Panel D. Log average establishment size, state-decade panel				
Log average establishment size	-0.723**	-0.019***	0.005	-1.080***
	(0.353)	(0.007)	(0.003)	(0.366)

Notes: The unit of observation is a U.S. state. Flow parameters are estimated separately by state and decade using the procedure described in the main text. The employment share of 100+ estab. is the employment share of establishments with 100 or more employees. Non-compete coverage is the share of workers reporting being bound by a non-compete agreement. In Panels A–B, the dependent variables are within-state changes in the corresponding flow parameter between the 1980s and 2010s; regressors are the within-state change in the indicated concentration measure and the contemporaneous non-compete share. Panels C–D use a state–decade panel with state and decade fixed effects and include only the concentration measure. Panels C–D cluster standard errors at the state level. Standard errors do not account for sampling uncertainty in the first-stage estimation of flow parameters. *Source:* CPS ASEC, BMS, and ORG, 1982–2021; BDS, 1982–2021; the SHED, 2022–2024.

the monthly arrival rate of directed outside offers, corresponding to roughly 10 percent of its level in the 1980s. As a point of reference, Berger et al. (2023) estimate that a one standard deviation increase in employer concentration (measured by the Herfindahl index) is associated with a 10 percent fall in the job-to-job mobility rate across local labor markets in Norway.

As for non-competes, Lipsitz and Starr (2022) estimate that a 2008 ban on non-competes for hourly and low-wage workers in Oregon raised monthly job-to-job mobility by 12–18 percent. Prior to the reform, 14 percent of such workers were bound by a non-compete, close to the 12 percent unweighted average across states in our sample. If we interpret a ban as reducing non-compete coverage from 12 percent to zero, our estimates imply an increase of $(-0.032) \times (-0.12) = 0.38$ percentage points in the monthly arrival rate of directed outside offers, of roughly 15 percent of its 1980s level. We stress with respect to both of these comparisons that we focus on the estimated arrival rate of *directed* outside offers, whereas these papers analyze realized job-to-job mobility. Realized job-to-job mobility falls by less than the decrease in λ^e for two reasons. First, as

λ^e falls, workers become worse matched, which raises the likelihood of accepting a given outside offer. Second, directed upward job mobility is only a subset of overall job-to-job mobility. We conclude that our estimates are in line with, or conservative relative to, existing evidence.

A simple back-of-the-envelope calculation helps put these estimates in perspective. Log average establishment size increased by about 0.08 nationally between the 1980s and 2010s, while 13 percent of workers report being covered by a non-compete agreement in 2022–2024. Combining these changes with the estimates in Table 6 implies a decline in employed-search efficiency of

$$0.08 \times 1.20 + 0.13 \times 1.83 \approx 0.33,$$

corresponding to roughly 63 percent of the estimated fall in ϕ^e from 1.25 to 0.72 in Table 2. Similarly, the employment share at 100+ establishments rose from 43.3% to 45.8% between the 1980s and 2010s. Combining this change with the estimates in Table 6 implies a decline in employed-search efficiency equal to roughly 59% of its estimated fall. This calculation is purely illustrative: it treats the cross-state coefficients as causal and abstracts from general-equilibrium feedback at the national level. Nevertheless, it suggests that rising concentration and non-compete use could account for a sizable share of the decline in employed-search efficiency.

6 The Aggregate Consequences of the Decline of the U.S. Job Ladder

In this section, we return to our original motivation: quantifying the role of changes to the structure of the U.S. labor market toward wage stagnation over the past 40 years.

6.1 Endogenizing the Offer Distribution

To translate the estimated decline in on-the-job search efficiency into aggregate wage dynamics, we now microfound the offer distribution following the seminal work of Burdett and Mortensen (1998). The economy has a unit mass of homogeneous workers and a mass m of heterogeneous firms that meet in a frictional labor market to produce a homogeneous good (with a price normalized to one). Workers earn a wage $w \geq w_0$ when employed and receive flow value b when nonemployed. Preferences are linear or logarithmic with discount rate ρ.

Workers' problem. A standard argument implies that nonemployed workers follow a reservation rule, accepting only offers paying $w \geq r$. With linear utility, the reservation wage solves

$$r = b + \left(p - \lambda^e - \lambda^f\right) \int_r^{\overline{w}} \frac{1 - F(w)}{\rho + \delta + \lambda^f + \lambda^e(1 - F(w))} dw, \tag{18}$$

while in the case of logarithmic preferences it is characterized by

$$\log r \quad = \quad \log b + \left(p - \lambda^e - \lambda^f\right) \int_r^{\overline{w}} \frac{1 - F(w)}{\rho + \delta + \lambda^f + \lambda^e(1 - F(w))} \frac{dw}{w}. \tag{19}$$

Let $w_0 = \max\{r, \underline{w}\}$ be the maximum of the reservation wage and a potential minimum wage.

Firms' problem. Firms differ in productivity z, distributed according to continuously differentiable CDF $\Gamma(z)$ over $[\underline{z}, \overline{z}]$. They post a wage w in order to maximize steady-state flow profits

$$\max_{w \geq w_0} \; (z + H(w) - w)\, l(w), \tag{20}$$

where $l(w)$ is the size a firm attains if it posts wage $w \geq w_0$ (see Burdett and Mortensen, 1998)

$$l(w) \quad = \quad \frac{p}{\delta + p} \frac{1 + \kappa}{(1 + \kappa(1 - F(w)))^2}.$$

The only non-standard part is $H(\cdot)$, which captures efficiency gains from higher pay. We assume $H(\cdot)$ is twice continuously differentiable and satisfies $H(w_0) = 0$ and $h(w) = H'(w) \in [0, 1)$.

Efficiency pay. To see why the data require $H(\cdot)$, consider the first-order condition to (20)

$$z(w) \quad = \quad w - H(w) + \frac{1 + \kappa(1 - F(w))}{2\kappa f(w)}(1 - h(w)). \tag{21}$$

In the baseline Burdett and Mortensen (1998) model ($H \equiv 0$), the thin empirical left tail implies high productivity among low-wage firms, and thus a counterfactually low labor share among such firms (Kehrig and Vincent, 2021). Moreover, differentiating (21)

$$z'(w) \quad = \quad \Big(1 - h(w)\Big) \left(\frac{1}{2} - \frac{1 + \kappa(1 - F(w))}{2\kappa f(w)} \frac{f'(w)}{f(w)}\right) - h'(w) \frac{1 + \kappa(1 - F(w))}{2\kappa f(w)}. \tag{22}$$

With $H \equiv 0$, the empirical offer distribution implies $z'(w) < 0$ below a threshold w_1, which as we show below is inconsistent with equilibrium (in principle there could be multiple such areas, but in practice there is one threshold). Bontemps, Robin and den Berg (2000) refer to wages below w_1 as *inadmissible*—there exists no productivity distribution such that the Burdett and Mortensen (1998) with $H(w) = 0$ can rationalize these outcomes. The threshold w_1 is given by

$$\kappa f(w_1)^2 \quad = \quad \Big(1 + \kappa(1 - F(w_1))\Big) f'(w_1). \tag{23}$$

Although several potential extensions could potentially resolve this shortcoming of the baseline model—including heterogeneity in the reservation wage (Burdett and Mortensen, 1998) or

endogenous search effort (Christensen et al., 2005)[20]—efficiency pay is tractable and has a long history in the literature (Shapiro and Stiglitz, 1984). We hence pursue this extension here. We normalize the least productive active firm to break even, $z(w_0) = w_0$, which together with a finite offer density at w_0 implies $h(w_0) = 1$. We restrict efficiency pay to the lower tail by setting $h(w) = 0$ for $w \geq w_1$, so that wages above w_1 are determined by the standard poaching and retention incentives in Burdett and Mortensen (1998).

6.2 The Impact of Lower Employed Search Efficiency in Theory

Let $w(z)$ denote the wage posted by a firm with productivity z. Assuming that wages are increasing in productivity ($w'(z) > 0$, verified below), we have $F(w(z)) = \Gamma(z)$. Using $f(w(z))w'(z) = \gamma(z)$ in (21), $w(z)$ solves for $z > z_0$ the first-order ODE

$$z = w(z) + \frac{1+\kappa(1-\Gamma(z))}{2\kappa\gamma(z)}w'(z) - \left(H(w(z)) + \frac{1+\kappa(1-\Gamma(z))}{2\kappa\gamma(z)}w'(z)h(w(z))\right),$$

subject to $w(z_0) = w_0$. Since the least productive firm breaks even, $z_0 = w_0$, the solution is

$$w(z) - H(w(z)) = z - \int_{w_0}^{z}\left(\frac{1+\kappa(1-\Gamma(z))}{1+\kappa(1-\Gamma(x))}\right)^2 dx. \tag{24}$$

Differentiating this verifies the assumption that $w'(z) > 0$

$$w'(z) = \frac{2\kappa\gamma(z)}{1-h(w(z))}\int_{w_0}^{z}\frac{1+\kappa(1-\Gamma(z))}{(1+\kappa(1-\Gamma(x)))^2}dx. \tag{25}$$

Finally, using the fact that $f(w(z))w'(z) = \gamma(z)$ gives the offer density

$$f(w(z)) = \frac{1-h(w(z))}{2\kappa\int_{w_0}^{z}\frac{1+\kappa(1-\Gamma(z))}{(1+\kappa(1-\Gamma(x)))^2}dx}.$$

A change in employed-search efficiency, ϕ^e, affects pay through two channels. First, differentiating the wage policy (24), holding w_0 fixed, as under for instance a binding minimum wage

$$\underbrace{\left.\frac{\partial w(z)}{\partial \phi^e}\right|_{w_0 \text{ fixed}}}_{\text{competition channel}} = \underbrace{\frac{2a}{1-h(w(z))}\int_{w_0}^{z}\frac{1+\kappa(1-\Gamma(z))}{(1+\kappa(1-\Gamma(x)))^3}\left(\Gamma(z)-\Gamma(x)\right)dx}_{>0},$$

where $a \equiv p/(\delta+\lambda^f) > 0$. A higher ϕ^e concentrates workers higher on the ladder and raises quit risk, strengthening poaching and retention incentives. Through this *competition channel*, a higher search efficiency in employment incentivizes firms to raise pay. Second, ϕ^e affects the reservation

[20] Another common extension to the baseline model is to endogenize vacancy creation (Mortensen, 2003). Such an extension does not change the range of inadmissible wages.

wage r, potentially affecting the lowest admissible wage w_0 and the wage policy

$$\underbrace{\left.\frac{\partial w(z)}{\partial \phi^e}\right|_{\kappa \text{ fixed}}}_{\text{reservation channel}} = \underbrace{\frac{1}{1-h(w(z))}\left(\frac{1+\kappa(1-\Gamma(z))}{1+\kappa(1-\Gamma(r))}\right)^2}_{>0}\left(\underbrace{\left.\frac{\partial r}{\partial \phi^e}\right|_{w(z) \text{ fixed}}}_{\text{PE reservation channel}} + \underbrace{\left.\frac{\partial r}{\partial \phi^e}\right|_{w(z) \text{ only}}}_{\text{GE reservation channel}}\right).$$

This *reservation channel* in turn has two parts: a partial equilibrium effect under a fixed wage policy and a general equilibrium effect as firms adjust their pay policy in equilibrium.

To make progress, we focus on the case of linear utility, a small discount rate $\rho \to 0$ and no efficiency pay, $H(w) = 0$. Substituting $dw = w'(z)\,dz$ in (18), where $w'(z)$ follows from (25)

$$r = b + a \underbrace{(1-\phi^e-\phi^f)}_{\text{partial equilibrium channel}} \underbrace{\kappa \int_r^{\overline{z}} \left(\frac{1-\Gamma(z)}{1+\kappa(1-\Gamma(z))}\right)^2 dz}_{\text{general equilibrium channel}}. \tag{26}$$

Holding fixed firms' pay policy, an increase in ϕ^e implies a lower foregone option value of search associated with accepting employment. When $1 > \phi^e + \phi^f$, a fall in ϕ^e unambiguously raises the reservation wage through this partial equilibrium reservation channel

$$\underbrace{\left.\frac{\partial r}{\partial \phi^e}\right|_{w(z) \text{ fixed}}}_{\text{PE reservation channel}} = -\frac{a\kappa \int_r^{\overline{z}} \left(\frac{1-\Gamma(z)}{1+\kappa(1-\Gamma(z))}\right)^2 dz}{1 + a(1-\phi^e-\phi^f)\,\kappa\left(\frac{1-\Gamma(r)}{1+\kappa(1-\Gamma(r))}\right)^2}$$

If $\phi^e + \phi^f > 1$ on the other hand, the reservation wage may rise or fall through this channel.

However, the wages posted by firms also change, in turn affecting the option value of continued search. For instance, as $\kappa \to 0$, all firms converge toward offering r (Diamond, 1982), and the gain from waiting vanishes. Differentiating (26) with respect to κ holding fixed the partial equilibrium reservation channel gives the general equilibrium reservation channel

$$\underbrace{\left.\frac{\partial r}{\partial \phi^e}\right|_{w(z) \text{ only}}}_{\text{GE reservation channel}} = \frac{1}{\frac{1}{a(1-\phi^e-\phi^f)} + \kappa\left(\frac{1-\Gamma(r)}{1+\kappa(1-\Gamma(r))}\right)^2} \int_r^{\overline{z}} \frac{(1-\Gamma(z))^2\Big(1-\kappa(1-\Gamma(z))\Big)}{\Big(1+\kappa(1-\Gamma(z))\Big)^3} dz.$$

If $\kappa < 1$ and $\phi^e + \phi^f < 1$, a higher ϕ^e *raises* the reservation wage through the general equilibrium reservation channel. More generally, the sign of the reservation channel and hence the overall effect of a change in the efficiency of employed search on wages is a quantitative question, to which we turn next.

6.3 The Impact of Lower Employed Search Efficiency across Space

We start by comparing the model-implied effect of state differences in $(\delta, p, \kappa, \lambda^f)$ with the data. To that end, we first recover $(H(w), \gamma(z), \underline{w}, b, \tau)$ based on our nationwide estimates of $(\delta, p, \kappa, \lambda^f)$ and $F(w)$ pooling all years of data. Specifically, we first determine the threshold w_1 from (23). For $w < w_1$, the data require efficiency pay, but separating productivity from efficiency pay is not possible without additional structure.[21] We hence assume a linear relationship below w_1, $z(w) = (1-\beta)w_0 + \beta w$, and solve the ODE (21) subject to $H(w_0) = 0$ and $h(w_1) = 0$, which gives

$$H(w) = (1-\beta)(w - w_0) + \beta \int_{w_0}^{w} \left(\frac{1+\kappa(1-F(w))}{1+\kappa(1-F(x))} \right)^2 dx, \tag{27}$$

$$\beta = \frac{1}{2\kappa f(w_1) \int_{w_0}^{w_1} \frac{1+\kappa(1-F(w_1))}{(1+\kappa(1-F(x)))^2} dx}. \tag{28}$$

For $w > w_1$, we set $h(w) = 0$ and recover productivity $z(w)$ from (21). The density of firms follows from $\gamma(z(w)) = f(w)/z'(w)$, where $z'(w) = \beta$ for $w < w_1$ and is given by (22) for $w > w_1$. Finally, we recover the flow value of nonemployment from (18)–(19) under the assumption of a five percent annual real interest rate. Three points deserve further discussion.

First, we only identify $H(w)$ for $w \geq w_0$, which complicates counterfactuals that shift the lower bound. If w_0 falls, we would need to extrapolate $H(w)$ below its identified range. If instead w_0 rises, and $h(w_0) \neq 1$, the implied wage density would counterfactually diverge at the new lower bound. To address both concerns, we assume efficiency pay is relative to the lowest admissible wage, $H(w) = \Psi(w - w_0)$, so firms enjoy some efficiency gains from paying more than strictly required. Because our estimates imply that the reservation wage tends to rise when ϕ^e falls, this conservative assumption dampens the implied decline in offered wages.

Second, we do not recover the underlying productivity distribution below z_0. If counterfactuals reduce the lowest admissible wage and shift z_0 left, the model requires assumptions about the left tail of $\gamma(z)$. We address this by extrapolating the inferred $\gamma(z)$ below z_0.

Third, we can infer the flow value of nonemployment b only when the reservation wage binds. We therefore do not consider counterfactuals in which the minimum wage binds in estimation but the reservation wage binds in counterfactuals. Instead, we focus on three scenarios: (i) a binding minimum wage throughout, $w_0 = \underline{w}$; (ii) a binding reservation wage with fixed b, $w_0 = r$; and (iii) a binding reservation wage with b equal to a fixed replacement rate τ of average wages. Having recovered $(\Psi(w - w_0), \gamma(z), \underline{w}, b, \tau)$ at the national level, we feed in state-level estimates $(\delta_s, p_s, \kappa_s, \lambda_s^f)$, holding fixed $\Psi(w - w_0)$ and $\gamma(z)$, and imposing either a binding, fixed minimum wage $\underline{w}$, or a binding reservation wage with either a fixed b or a fixed τ.

[21] In practice, for numerical stability we impose $h(w) > 0$ for $w < w_1 + \varepsilon$ for some small ε.

Figure 9: Average Offered Residual Wage (Top) and Average Earned Wage (Bottom)

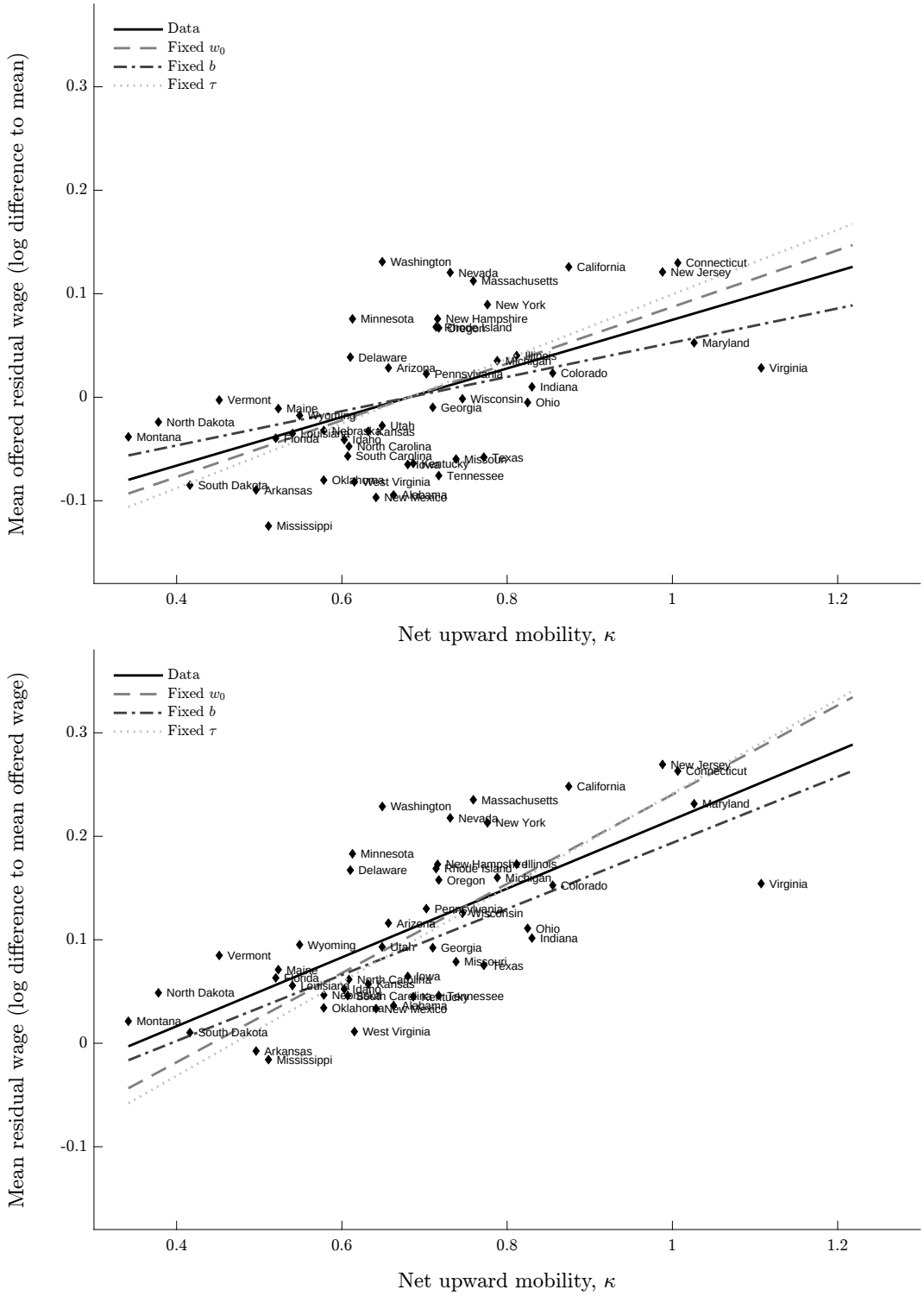

Notes: The unit of observation is a U.S. continental state. Wages are residuals that control for gender, race, education, and 3-digit occupation fully interacted with year, and are deflated by the average residual wage of an age-matched hire from nonemployment. Mean offered wages are expressed as deviations from their cross-state mean. Mean earned wages are expressed as deviations from the cross-state mean of *offered* wages. Fixed w_0 assumes a binding minimum wage. Fixed b assumes a binding reservation wage with a fixed flow value of nonemployment. Fixed τ assumes a binding reservation wage with a fixed replacement rate. *Source:* CPS BMS and ORG 1982–2021, and authors' calculations.

Figure 9 plots mean offered and earned residual wages in the data and model against net upward job mobility under log utility. Residual wages are constructed as earlier, except that we omit state–time fixed effects. In both the data and the model, offered wages in the top panel are higher in high-κ states. As we noted above, greater upward job mobility incentivizes firms to post higher wages to poach and retain workers. With a fixed minimum wage, this competition channel is the only force, so offered wages rise unambiguously with κ. When the reservation wage binds, higher employed-search efficiency can also lower the reservation wage, putting downward pressure on offered pay. This reservation channel is stronger under fixed b than under a fixed replacement rate τ, because maintaining a constant τ requires b to rise with earned wages in high-κ states. Overall wages in the bottom panel are also higher in high-κ states as workers move up the job ladder more. Yet in the data as well as most specifications of the model, the higher wages in high-κ states are primarily accounted for by higher offered wages, not greater wage gains from subsequent upward job mobility.

Appendix D.1 shows that the labor share is also higher in high-κ states in both the model and the data, although the model understates the empirical relationship. We also find no relationship between upward job mobility and two other potential drivers of wages: state minimum wages and UI replacement rates. Such confounding factors do not account for the patterns in Figure 9.

Appendix D.2 shows that these patterns are less pronounced under linear utility, because log preferences limit the desire to wait for a very good offer. Nevertheless, the reservation channel is never strong enough to overturn the competition channel. Appendix D.2 also reports additional outcomes that are counterfactual under linear utility, leading us to prefer log utility.

6.4 The Impact of Lower Employed Search Efficiency over Time

We finally turn to the time series to quantify how changes in labor-market structure have contributed to wage stagnation over the past four decades. Let $Z_d(i) = e^{A_d} z$ denote firm i's productivity in decade d, where A_d is an aggregate productivity shifter and z is the firm's *relative* productivity. Relative productivity follows decade-specific density $\gamma_d(z)$, normalized to have mean zero in logs, $\int z \ln z \, d\Gamma_d(z) = 0$ for all d. The flow value of nonemployment is $B_d = e^{A_d} b_d$, the minimum wage is $\underline{W}_d = e^{A_d} \underline{w}_d$, and the replacement rate is τ_d. Finally, $(\delta_d, p_d, \kappa_d, \lambda_d^f)$ summarize labor-market structure in decade d. We recover $(H_d(w), \gamma_d(z), \underline{w}_d, b_d, \tau_d)$ following the same steps as above. We also recover the aggregate TFP shifter A_d to match the trend in composition-adjusted real wage growth in Figure 1. Finally, we construct $\Psi_d(w - w_0)$ from $H_d(w)$ and w_0.

Figure 10 summarizes key model outcomes in the 1980s and 2010s (the other decades are convex combinations). As expected, the model replicates the offer distribution in both decades in panel (a). Composition-adjusted real offered wages rise by 8.2 log points over this period, while composition-adjusted real wages rise by 1.0 log point (panel (b)). Efficiency pay considerations matter for roughly 15 percent of workers, with wage setting for most workers being governed by

the poaching and retention incentives emphasized by Burdett and Mortensen (1998) (panel (c)).

The estimated productivity distribution $\gamma(z)$ has a rising lower tail and a long right tail. Between the 1980s and 2010s, average efficiency gains rose by 10.6 log points and average (unweighted) firm productivity by 33.8 log points. Aside from a rightward shift, the shapes of the efficiency-pay schedule and the productivity distribution change little. That is, the shrinking dispersion in offered wages in panel (a) is not the result of less dispersed productivity, but due to less efficient search on-the-job that lead high-productivity firms to pay less.

The outcomes in panels (a)–(c) are independent of the utility function and therefore do not identify it. However, the utility specification matters for counterfactuals. To discriminate between log and linear utility, Figure 10d compares the implied replacement rate under both specifications with the data (rescaled to match the 1980s level, which is around 0.3–0.5). In the data, the replacement rate is roughly stable until the last decade, when it declines. The model requires a larger fall in the replacement rate to rationalize the reservation wage in the face of declining employed-search efficiency. Moreover, linear utility amplifies this force by making workers more willing to wait in nonemployment. Based on this evidence, we prefer the log-utility specification.

Table 7 reports our time-series decomposition. Between the 1940s and 1970s, composition-adjusted real wages grew at 2.08 percentage points per year, broadly in line with productivity. As a first counterfactual, we let aggregate TFP follow its estimated path while holding fixed at their 1980s values: (i) the efficiency-pay schedule and productivity distribution, $(\Psi(w - w_0), \gamma(z))$; (ii) the parameters governing the lowest admissible wage, $(\underline{w}, b, \tau)$—i.e., we assume $(\underline{W}_d = e^{A_d}\underline{w}, , B_d = e^{A_d}b)$ grow with productivity; and (iii) the labor-market structure $(\delta, p, \kappa, \lambda^f)$. Under this experiment, composition-adjusted real wages would have grown by 1.13 percentage points per year between the 1980s and 2010s. Given that realized annual wage growth was 0.03 percentage points between the 1980s and 2010s, a deceleration in aggregate TFP growth accounts for $(2.08 - 1.13)/(2.08 - 0.03) \approx 46$ percent of the overall decline in wage growth between the earlier and later parts of our sample.

Next, we also allow the structure of the labor market $(\delta, p, \kappa, \lambda^f)$ to evolve as estimated, while still holding fixed the efficiency-pay schedule, the productivity distribution, and the objects governing the reservation wage, $(\underline{w}, b, \tau)$. In this case, composition-adjusted real wages would have grown by 0.42–0.94 percentage points per year. Relative to the TFP-only benchmark, changes in labor-market structure therefore imply an additional $1.13 - 0.94 = 0.19$ to $1.13 - 0.42 = 0.71$ percentage-point decline in annual wage growth. The effect is smallest under linear utility with a fixed flow value of nonemployment, because the declining efficiency of employed search results in a sharp rise in the reservation wage, offsetting the competition effect. We note, however, that this specification (linear utility with fixed b) implies too large a decline in the replacement rate (Figure 10d) and is inconsistent with the cross-state evidence (Figure D.13). The effect is largest under a binding minimum wage, since this shuts down any adjustment of the reservation wage.

Under our preferred specification with log utility and a fixed replacement rate—which matches

Figure 10: Model Estimates

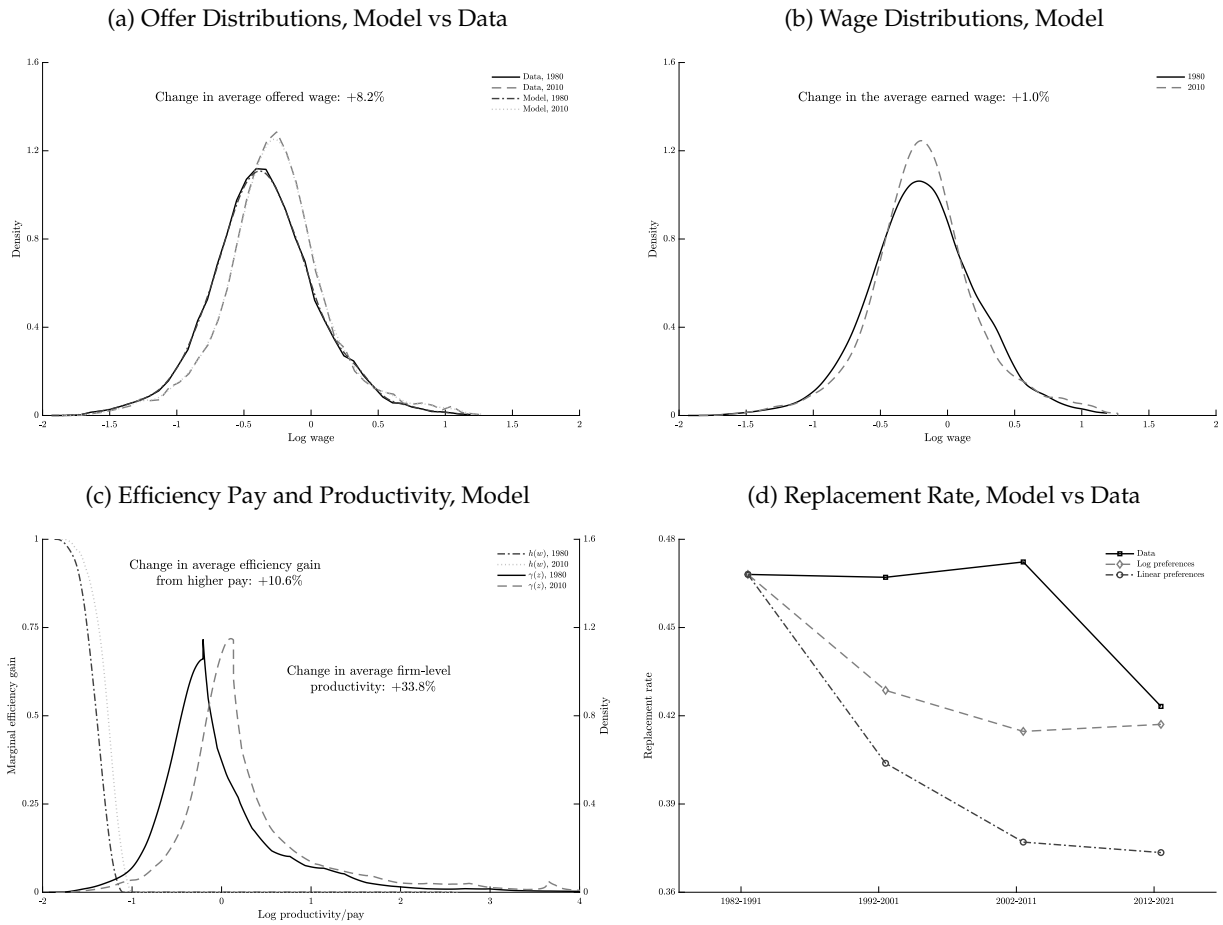

Notes: Panel (a) plots the distribution of composition-adjusted real wages of hires from nonemployment in the model and data. Panel (b) plots the distribution of composition-adjusted real wages of in the model and data. Panel (c) plots the estimated marginal efficiency gain from paying more, $h(w)$, together with the firm productivity distribution $\gamma(z)$. Panel (d) plots the replacement rate, defined as the flow value of nonemployment divided by average wages. *Source:* CPS BMS and ORG 1982–2021 and authors' calculations.

best the behavior of the replacement rate in Figure 10d as well as the cross-state evidence in Figure D.10—composition-adjusted real wage growth falls to 0.45 percentage points per year between the 1980s and 2010s. Relative to the TFP-only benchmark of 1.13, this implies that changes in labor-market structure have reduced annual wage growth by an additional $1.13 - 0.45 = 0.68$ percentage points, which corresponds to about $0.68/(2.08 - 0.03) \approx 33$ percent of the overall slowdown in annual wage growth between the 1940s–1970s and the 1980s–2010s. Figure 11 illustrates this case. The remaining slowdown is mostly accounted for by a falling replacement rate (see Figure 10d), with changes in the shape of the efficiency-pay schedule and the productivity distribution playing only a minor role.

Table 7: Annualized Real Wage Growth (percentage points).

Realized annual wage growth between 1940 and 1970	2.08	
Counterfactual wage growth between 1980s and 2010s	Log	Linear
Changing TFP only, fixed $(\Phi(w-w_0), \gamma(z))$, $(\underline{w}, b, \tau)$ and $(\delta, p, \kappa, \lambda^f)$	1.13	
Changing TFP and labor market structure $(\delta, p, \kappa, \lambda^f)$		
Binding $\underline{w}$	0.42	
Binding r with fixed b	0.64	0.94
Binding r with fixed τ	0.45	0.70
Realized annual wage growth between 1980s and 2010s	0.03	

Notes: The table reports model-implied wage growth in response to changing $(A, \delta, p, \kappa, \lambda^f)$ from their 1980s to 2010s values, holding fixed efficiency pay $\Phi(w-w_0)$, the productivity distribution $\gamma(z)$ and $(\underline{w}, b, \tau)$. The three scenarios differ in how the lowest admissible wage adjusts: (i) the minimum wage is binding and w_0 is held fixed, (ii) the reservation wage is binding and b is held fixed, and (iii) the reservation wage is binding and the replacement rate $\tau \equiv b/\overline{w}$ is held fixed (with $\overline{w}$ denoting the average earned wage). *Source:* U.S. Decennial Census 1940–1960; CPS ASEC 1962–2021; CPS BMS and ORG 1982–2021; and authors' calculations.

7 Conclusion

Real wage growth in the United States has been markedly weaker over the past four decades than in the earlier postwar period. This paper argues that part of this wage stagnation reflects changes in the structure of the U.S. labor market and the associated decline in upward job mobility. We show that the gap between the cross-sectional wage and offer distributions has narrowed substantially since the 1980s, indicating declining upward job mobility.

The sharp fall in upward job mobility, combined with only a modest decline in the job-finding rate of the nonemployed, is inconsistent with explanations such as a decline in aggregate matching efficiency, labor demand, or changes in workers' acceptance behavior. Instead, it points to forces that have reduced the efficiency of on-the-job search. Using long-run cross-state variation, we provide new evidence that rising employer concentration and the increased use of noncompete agreements have played an important role in reducing the efficiency of employed search.

We end by quantifying the aggregate wage implications of the estimated changes to the structure of the U.S. labor market using a wage-posting model in the spirit of Burdett and Mortensen (1998). A decline in on-the-job search efficiency induces firms to lower offered wages, since they are more likely to hire at a given wage and less likely to lose workers to competing firms. At the same time, workers' reservation wage rises, as accepting employment entails giving up a higher option value of continued search. Under our preferred estimate, the former effect dominates, with the decline in employed search efficiency accounting for a third of the postwar slowdown in real wage growth.

Figure 11: Counterfactual Real Wages in the United States, 1940–2020

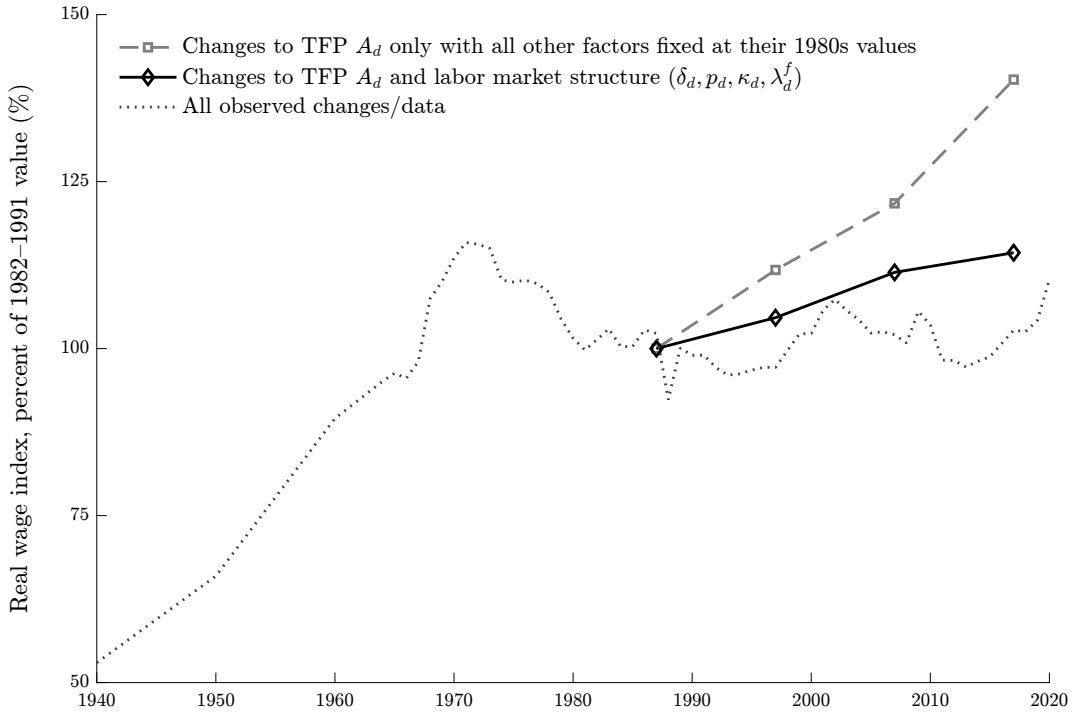

Notes: Changes to TFP only lets aggregate TFP A_d change as estimated, holding fixed: (i) the shape of the efficiency pay schedule $\Phi(w - w_0)$ and productivity distribution $\gamma(z)$; (ii) the factors governing the lowest admissible wage $(\underline{w}, b, \tau)$; and (iii) the structure of the labor market $(\delta, p, \kappa, \lambda^f)$. Changes to TFP and labor market structure lets also $(\delta, p, \kappa, \lambda^f)$ evolve as estimated. Model outcomes are based on the fixed replacement rate scenario. Data series holds fixed the demographic composition along age, gender, race and education fixed at its level in 1982. *Source:* U.S. Decennial Census 1940–1960; CPS ASEC 1962–2021; CPS BMS and ORG 1982–2021; and authors' calculations.

References

Abowd, John M., and Arnold Zellner. 1985. "Estimating Gross Labor-Force Flows." *Journal of Business and Economic Statistics*, 3: 254–283.

Acemoglu, Daron. 2002. "Technical Change, Inequality, and the Labor Market." *Journal of Economic Literature*, 40(1): 7–72.

Acemoglu, Daron, and Pascual Restrepo. 2020. "Robots and Jobs: Evidence from US Labor Markets." *Journal of Political Economy*, 128(6): 2188–2244.

Autor, David, Arindrajit Dube, and Annie McGrew. 2023. "The unexpected compression: Competition at work in the low wage labor market." National Bureau of Economic Research.

Autor, David H. 2015. "Why Are There Still So Many Jobs? The History and Future of Workplace Automation." *Journal of Economic Perspectives*, 29(3): 3–30.

Autor, David H., David Dorn, and Gordon H. Hanson. 2013. "The China Syndrome: Local Labor Market Effects of Import Competition in the United States." *American Economic Review*, 103(6): 2121–2168.

Azar, José, Ioana Marinescu, and Marshall Steinbaum. 2022. "Labor market concentration." *Journal of Human Resources*, 57(S): S167–S199.

Azar, José, Ioana Marinescu, Marshall Steinbaum, and Bledi Taska. 2020. "Concentration in US labor markets: Evidence from online vacancy data." *Labour Economics*, 66: 101886.

Bagga, Sadhika. 2023. "Firm Market Power, Worker Mobility, and Wages in the US Labor Market." *Journal of Labor Economics*, 41: 205–256.

Benmelech, Efraim, Nittai K. Bergman, and Hyunseob Kim. 2022. "Strong Employers and Weak Employees: How Does Employer Concentration Affect Wages?" *Journal of Human Resources*, 57: S200–S250.

Berger, David, Kyle Herkenhoff, and Simon Mongey. 2022. "Labor Market Power." *American Economic Review*, 112(4): 1147–93.

Berger, David W, Kyle F Herkenhoff, Andreas R Kostøl, and Simon Mongey. 2023. "An Anatomy of Monopsony: Search Frictions, Amenities and Bargaining in Concentrated Markets." National Bureau of Economic Research Working Paper 31149.

Bontemps, Christian, Jean-Marc Robin, and Gerard J. Van den Berg. 2000. "Equilibrium Search with Continuous Productivity Dispersion: Theory and Nonparametric Estimation." *International Economic Review*, 41(2): 305–358.

Burdett, Kenneth, and Dale T Mortensen. 1998. "Wage differentials, employer size, and unemployment." *International Economic Review*, 257–273.

Caldwell, Sydnee, and Oren Danieli. 2024. "Outside Options in the Labour Market." *The Review of Economic Studies*, rdae006.

Card, David, and John E. DiNardo. 2002. "Skill-Biased Technological Change and Rising Wage Inequality: Some Problems and Puzzles." *Journal of Labor Economics*, 20(4): 733–783.

Christensen, Bent Jesper, Rasmus Lentz, Dale T. Mortensen, George R. Neumann, and Axel Werwatz. 2005. "On-the-Job Search and the Wage Distribution." *Journal of Labor Economics*, 23(1): 31–58.

Clark, Kim B, and Lawrence H Summers. 1979. "Labor Market Dynamics and Unemployment: A Reconsideration." *Brookings Papers on Economic Activity*, 1979(1): 13–72.

Diamond, Peter A. 1982. "Wage Determination and Efficiency in Search Equilibrium." *Review of Economic Studies*, 49: 217–227.

Faberman, Jason R, Andreas I Mueller, Ayşegül Şahin, and Giorgio Topa. 2022. "Job Search Behavior Among the Employed and Non-employed." *Econometrica*, 90: 1743–1779.

Fallick, Bruce, and Charles A. Fleischman. 2004. "Employer-to-Employer Flows in the U.S. Labor Market: The Complete Picture of Gross Worker Flows." Board of Governors of the Federal Reserve System (U.S.) Finance and Economics Discussion Series 2004-34.

Farber, Henry S., Daniel Herbst, Ilyana Kuziemko, and Suresh Naidu. 2018. "Unions and Inequality Over the Twentieth Century: New Evidence from Survey Data."

Flood, Sarah M., and José D. Pacas. 2017. "Using the Annual Social and Economic Supplement as part of a Current Population Survey panel." *Journal of Economic and Social Measurement*, 42(3-4): 225–248. PMID: 29937619.

Fujita, Shigeru, and Giuseppe Moscarini. 2017. "Recall and Unemployment." *American Economic Review*, 107(12): 3875–3916.

Fujita, Shigeru, Giuseppe Moscarini, and Fabien Postel-Vinay. 2024. "Measuring employer-to-employer reallocation." *American Economic Journal: Macroeconomics*, 16(3): 1–51.

Gottfries, Axel, and Gregor Jarosch. 2023. "Dynamic Monopsony with Large Firms and Noncompetes." Working Paper.

Haltiwanger, John, Henry Hyatt, and Erika McEntarfer. 2018. "Who moves up the job ladder?" *Journal of Labor Economics*, 36(S1): S301–S336.

Jolivet, Gregory, Fabien Postel-Vinay, and Jean-Marc Robin. 2006. "The empirical content of the job search model: Labor mobility and wage distributions in Europe and the US." *Contributions to Economic Analysis*, 275: 269–308.

Kehrig, Matthias, and Nicolas Vincent. 2021. "The Micro-Level Anatomy of the Aggregate Labor Share Decline." *Quarterly Journal of Economics*.

Lee, David S. 1999. "Wage Inequality in the United States During the 1980s: Rising Dispersion or Falling Minimum Wage?" *The Quarterly Journal of Economics*, 114(3): 977–1023.

Lipsitz, Michael, and Evan Starr. 2022. "Low-Wage Workers and the Enforceability of Noncompete Agreements." *Management Science*, 68(1): 143–170.

Mortensen, Dale T. 2003. *Wage Dispersion: Why Are Similar Workers Paid Differently?* Cambridge, MA:MIT Press.

Ozkan, Serdar, Jae Song, and Fatih Karahan. 2023. "Anatomy of Lifetime Earnings Inequality: Heterogeneity in Job-Ladder Risk versus Human Capital." *Journal of Political Economy Macroeconomics*, 1(3): 506–550.

Petrongolo, Barbara, and Christopher A. Pissarides. 2001. "Looking into the Black Box: A Survey of the Matching Function." *Journal of Economic Literature*, 39(2): 390–431.

Postel-Vinay, Fabien, and Jean-Marc Robin. 2002. "Equilibrium Wage Dispersion with Worker and Employer Heterogeneity." *Econometrica*, 70(6): 2295–2350.

Prager, Elena, and Matt Schmitt. 2021. "Employer Consolidation and Wages: Evidence from Hospitals." *American Economic Review*, 111(2): 397–427.

Rinz, Kevin. 2022. "Labor Market Concentration, Earnings, and Inequality." *Journal of Human Resources*, 57(S): S251–S283.

Shapiro, Carl, and Joseph E. Stiglitz. 1984. "Equilibrium Unemployment as a Worker Discipline Device." *American Economic Review*, 74(3): 433–444.

Starr, Evan P., J. J. Prescott, and Norman D. Bishara. 2021. "Noncompete Agreements in the U.S. Labor Force." *Journal of Law and Economics*, 64(1): 53–84.

Topel, Robert H, and Michael P Ward. 1992. "Job mobility and the careers of young men." *Quarterly Journal of Economics*, 107(2): 439–479.

A Data Appendix

In this section, we provide additional details about our microdata and the process we use to clean the data.

A.1 Allocation Rates in the CPS

We now describe our procedure for assigning consistent demographics within individuals, necessitated by a high and rising share of allocated demographic information for households in the CPS. We focus on individuals aged at least 20, since allocation rates are particularly high for younger individuals who do not enter our sample at any point, and at most 65, since such individuals do not enter our analysis sample. We also exclude individuals who are missing age, race, or sex from this analysis, since it is impossible to benchmark them appropriately[22].

Figure A.1 shows the rapid increase in the share of jobs which have allocated values of demographics. Figure A.2 shows that since 1994, there has been a large increase in the share of individuals with at least some demographic information allocated, rising to nearly 10% of all observations by the 2020s (corresponding to about 90% of observations having no allocated data). These individuals tend to be associated with smaller samples with higher average demographic weights, making the weighted share of observations with some allocation even higher. This increase motivates our standardisation procedure for demographics within individuals. This procedure first replaces all allocated values of race, age and sex by missing values, and then proceeds to use non-allocated values to fill in the true race, sex and age. The tables below explore the validity of our procedure. For sex, our procedure sets sex missing in 44,803 observations, about 0.1% of the 41.6 million observations in total. For race, our procedure sets race missing for 1,224,174 observations (about 2.9% of the total) and reassigns 6,761 values (about 0.016% of the total).

We recode education to five categories using the IPUMS variable EDUC as a baseline, and using raw variables for the highest grade attended and for grade completion for years prior to 1992, accounting for changes in 1989 to the coding of these variables. We then standardise education to the highest level ever attained by an individual over their time in the sample. Our procedure produces 299,385 individuals (about 0.7% of observations) for whom we assign a lower highest recorded education level than in the raw data, which occurs whenever an individual has their highest education level be an allocated data point and also has unallocated values for lower education levels reported earlier. Finally, our procedure assigns a missing employment status to 603,419 observations with allocated employment status (about 1.4% of observations).

Table A.5 shows that our procedure does not affect the distribution of demographic variables in any of the decades we study, with only very minor differences in the 1992-2001 period. This period includes the 1994 CPS redesign and the change of the household numbering system in

[22]There are no individuals who are missing demographic information in some interview months but not in others.

Figure A.1: Shares of observations containing non-missing allocated values of sex, race, age and education over time. The left panel shows these shares weighted by the demographic weights, while the right panel shows the raw share of the number of observations with allocated demographics.

1995.

A.2 Demographic Composition of Final Dataset

In constructing our final dataset, we retain only individuals satisfying all of the following characteristics.

1. non-missing age, sex, race, education
2. aged between 20 and 59 years when they enter the sample
3. if listed as wage-employed, non-missing an occupation. We also construct a separate occupational indicator which imputes missing occupation using an individual's modal occupational indicator.
4. never earning a wage outside the 0.5th or 99.5th percentiles of the residual wage distribution pooled across all years[23].

[23]We construct residual wages with occupation controls, with occupation controls based on imputing missing occupations by the modal occupations within an individual, and without occupation controls. We construct the drop thresholds as the highest of the 0.5th percentiles of each of these three distributions, and the lowest of the 99.5th per-

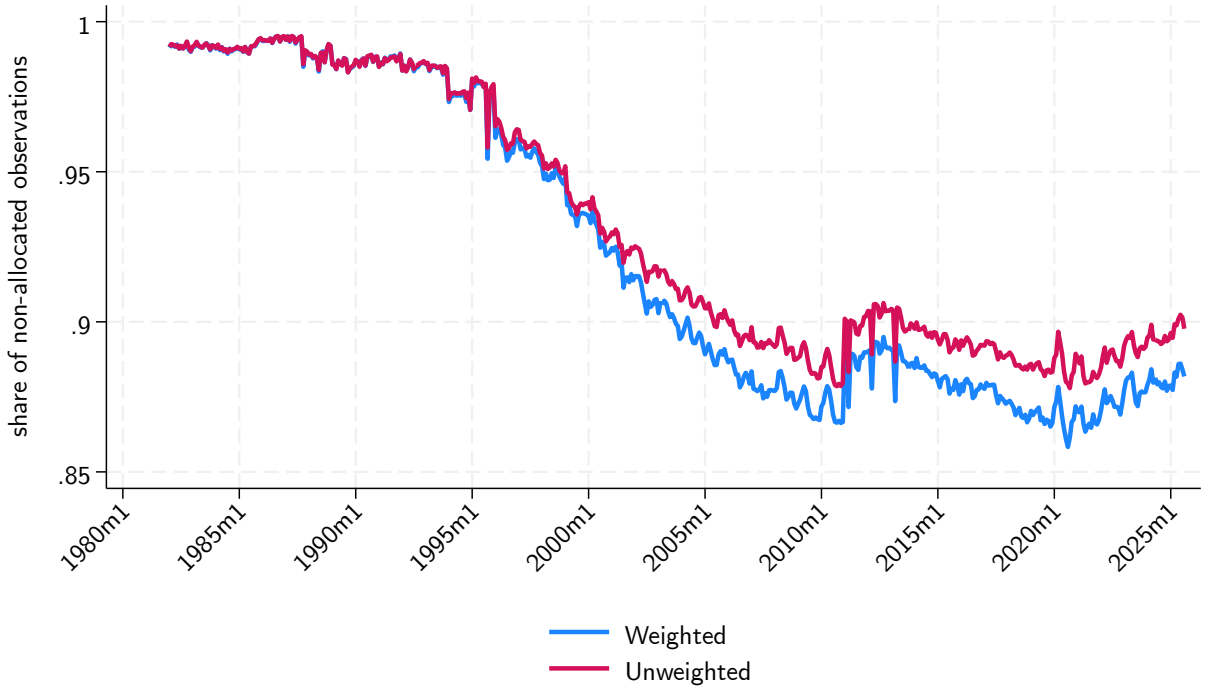

Figure A.2: Shares of observations containing no allocated values of sex, race, age, education or employment status over time.

Our procedure further harmonises employment status to classify individuals as being employed, non-employed or having a missing employment status.

A.3 Attrition in the CPS over the sample

Our empirical approach exploits the short panel dimension of the CPS, and in this section, we discuss attrition within the sample. All results below are based on the sample constructed applying our demographic restrictions.

Figure A.3 shows the share of workers who respond to survey $i+1$ conditional on responding to survey i, which we require to construct changes in employment status across individuals over time. Overall, attrition in the sample between adjacent months is quite low. However, there is substantial attrition between MIS 4 and MIS 5, which are 8 calendar months apart, with only about a fifth of all respondents being contactable. Reassuringly, this attrition remains stable over our sample period. Note that

- changes in the way household identifiers are constructed in June and September 1985 lead to households being unlinkable between their 4th and 13th BMS (i.e. between interviews MIS 4 and MIS 5) in 1985-86.

centiles of each of these three distributions.

		Reported Sex with Allocated Values			
	Male?	No	Yes	Missing	**Total**
Standardized Sex	No	21,490,432	0	0	**21,490,432**
	Yes	0	20,053,644	0	**20,053,644**
	Missing	20,914	23,889	0	**44,803**
	Total	**21,511,346**	**20,077,533**	**0**	**41,588,879**

Table A.1: Cross-tabulation of standardized and reported, allocated values for sex.

		Reported Race with Allocated Values			
	Race	White	Non-White	Missing	**Total**
Standardized Race	White	33,699,853	102	0	**33,699,955**
	Non-White	6,659	6,658,091	0	**6,664,750**
	Missing	1,026,117	198,057	0	**1,224,174**
	Total	**34,732,629**	**6,856,250**	**0**	**41,588,879**

Table A.2: Cross-tabulation of standardized and reported, allocated values for race. The non-white race category pools all other racial categories.

- changes in household identifier construction in May 1995 lead to much lower linkage rates for these months. Linkage rates in these months are also affected by the introduction of the new sample in 1994.
- starting in September 2000, the CPS expanded the monthly sample by about 10,000 new households over a three-month period.
- changes in age topcodes in February 2002 and April 2004 affect match rates in the early 2000s due to age validation being a requirement of the construction of CPSIDV, even with allowances made for the higher topcodes (Flood and Pacas, 2017).
- in April 1984, April 1994, April 2004 and April 2014, a new CPS sample is introduced following the decennial census immediately preceding it. This leads to a drop in the MIS4-5 linkage rate across these periods, which affects the cohorts entering 8-12 months prior to these dates. Changes introduced in April of year t continue to affect the sample until July of year $t+1$.

Figure A.4 displays the share of individuals responding to the second ORG survey conditional on responding to the first. We see that this share largely follows the share of individuals we can track across cohorts, reflecting the fact that the main point of attrition in the CPS is the 8-month period between MIS 4 and MIS 5 (i.e. months 4 and 13).

		Highest Reported Education with Allocated Values						
	Education	LTHS	HSD	SCLG	BACH	CLG+	Missing	Total
Standardized Education	LTHS	4,703,763	42,598	31,356	21,384	10,983	0	**4,810,084**
	HSD	0	12,974,360	62,079	43,310	23,203	0	**13,102,952**
	SCLG	0	0	11,384,724	32,981	16,932	0	**11,434,637**
	BACH	0	0	0	7,701,212	14,559	0	**7,715,771**
	CLG+	0	0	0	0	3,971,591	0	**3,971,591**
	Missing	58,954	157,139	136,696	103,611	54,884	42,560	**553,844**
	Total	**4,762,717**	**13,174,097**	**11,614,855**	**7,902,498**	**4,092,152**	**42,560**	**41,588,879**

Table A.3: Cross-tabulation of standardized and reported, allocated highest education levels. Key: LTHS = Less than high school, HSD = High school diploma, SCLG = Some college, BACH = Bachelor's degree, CLG+ = More than a bachelor's degree.

		Reported Employment Status with Allocated Values						
	Status	Wage, Pvt	Wage, Pub	Self-Emp	Unemp	NILF	Missing	Total
Standardized Employment	Wage, Pvt	21,613,063	0	0	0	0	0	21,613,063
	Wage, Pub	0	4,839,425	0	0	0	0	4,839,425
	Self-Emp	0	0	3,364,636	0	0	0	3,364,636
	Unemp	0	0	0	1,606,605	0	0	1,606,605
	NILF	0	0	0	0	9,561,731	0	9,561,731
	Missing	266,540	74,817	55,016	49,950	67,261	89,835	603,419
	Total	**21,879,603**	**4,914,242**	**3,419,652**	**1,656,555**	**9,628,992**	**89,835**	**41,588,879**

Table A.4: Cross-tabulation of standardized and reported, allocated employment status. Key: Wage, Pvt = Wage employed, private; Wage, Pub = Wage employed, public; Self-Emp = Self-employed; Unemp = Unemployed; NILF = Not in labor force. The final column shows the number of off-diagonal observations for each standardized category.

A.4 Implications of Allocation in Wages

The left panel of figure A.5 shows that a substantial share of all wage observations in the CPS are allocated, raising questions about measurement error. The right panel shows that in practice, the distribution of allocated wages is close enough to the distribution of actual wages to leave the mean wage virtually unchanged. The pooled correlation between the distributions of residual wages and residual allocated wages is over 99%.

A.5 Share who Forget About Event

Figure A.6 plots the share of workers who report to be a job stayer during the year in the March supplement by the month in which they previously reported in their BMS survey to be non-employed. The more time that has passed between the spell of non-employment and the March

	1982-1991		1992-2001		2002-2011		2012-2021	
	Raw	Std	Raw	Std	Raw	Std	Raw	Std
A. Sex and Race								
Male	0.485	0.485	0.489	0.489	0.492	0.492	0.490	0.490
White	0.855	0.855	0.831	0.831	0.805	0.807	0.770	0.771
B. Education								
LTHS	0.182	0.181	0.134	0.132	0.109	0.105	0.082	0.077
HSD	0.373	0.373	0.329	0.328	0.296	0.293	0.270	0.266
SCLG	0.233	0.233	0.285	0.286	0.298	0.299	0.298	0.298
BACH	0.144	0.145	0.171	0.172	0.199	0.202	0.228	0.232
CLG+	0.069	0.069	0.081	0.082	0.099	0.101	0.123	0.126
C. Age								
20-29	0.283	0.283	0.233	0.233	0.221	0.221	0.221	0.221
30-39	0.266	0.266	0.270	0.270	0.222	0.222	0.213	0.214
40-49	0.189	0.189	0.241	0.241	0.242	0.242	0.208	0.207
50-59	0.153	0.153	0.163	0.163	0.208	0.208	0.219	0.219
D. Employment Status								
Employed	0.629	0.629	0.660	0.660	0.645	0.647	0.644	0.643
Nonemployed	0.290	0.290	0.257	0.256	0.277	0.275	0.287	0.287

Table A.5: Distribution of demographic characteristics in each period of our analysis. The Raw and Std columns respectively contain the distributions with allocated variables, and omitting allocated variables and standardising demographics within individuals. Totals may not add up to 1 due to rounding. For employment status, the remaining share of observations is accounted for by the self-employed and "missing" categories; we drop the self-employed in our main analysis and explicitly account for missing employment status in our empirical exercises.

survey, the more likely a respondent is to misreport their status.

	1982-1991	1992-2001	2002-2011	2012-2021
A. Sex and Race				
Male	0.485	0.488	0.490	0.489
White	0.856	0.831	0.807	0.772
B. Education				
LTHS	0.183	0.131	0.096	0.069
HSD	0.373	0.330	0.294	0.265
SCLG	0.230	0.283	0.301	0.300
BACH	0.145	0.173	0.206	0.237
CLG+	0.069	0.083	0.103	0.129
C. Age				
20-29	0.286	0.233	0.218	0.220
30-39	0.268	0.271	0.219	0.211
40-49	0.190	0.243	0.244	0.207
50-59	0.154	0.165	0.213	0.223
D. Employment Status				
Employed	0.627	0.659	0.648	0.650
Nonemployed	0.292	0.256	0.272	0.280

Table A.6: Distribution of demographic characteristics in each period of our analysis in the final dataset. Totals may not add up to 1 due to rounding. For employment status, the remaining share of observations is accounted for by the "missing" category; we explicitly account for missing employment status in our empirical exercises.

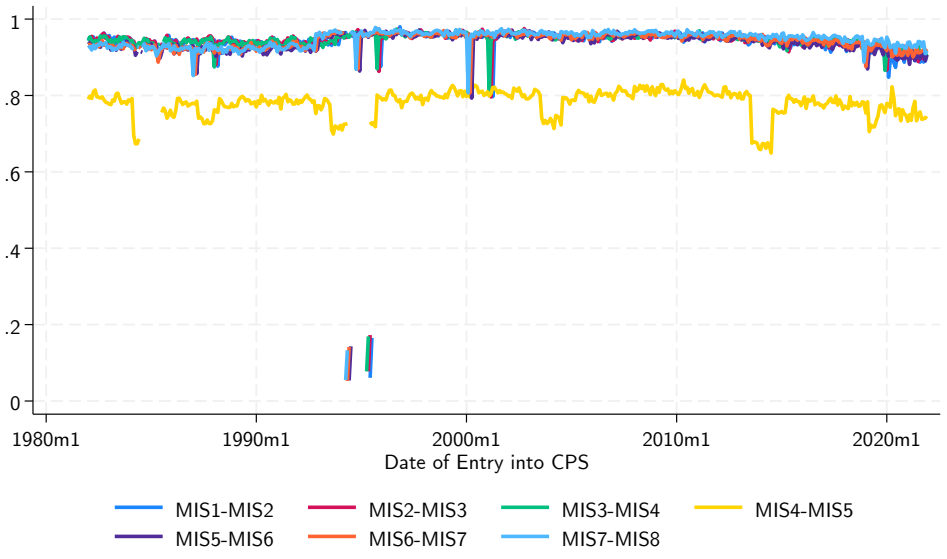

Figure A.3: Share of individuals responding to survey $i+1$ conditional on responding to survey i across entering cohorts.

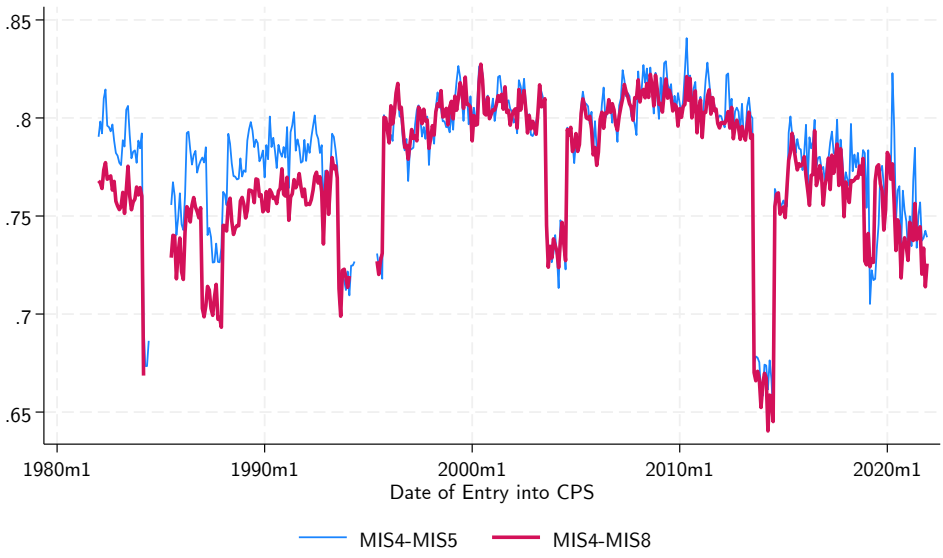

Figure A.4: Share of individuals responding to survey 8 conditional on responding to survey 4 across entering cohorts.

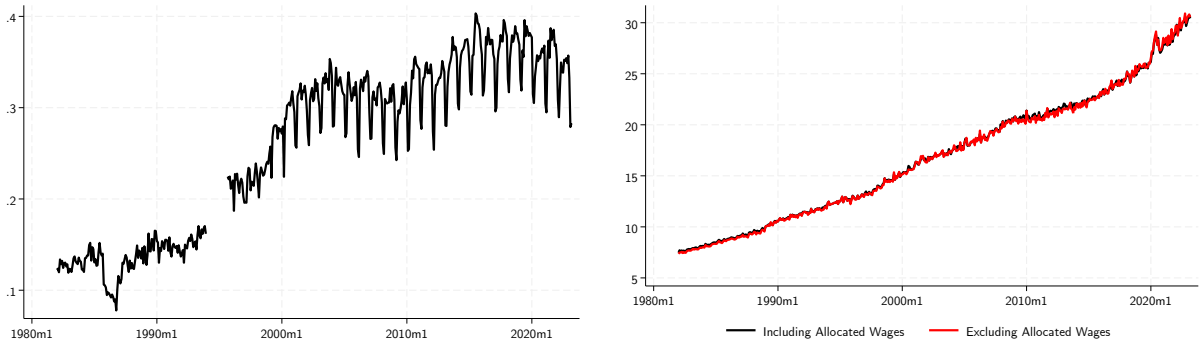

Figure A.5: LEFT: Share of observations with a valid wage which are allocated. RIGHT: Mean wage levels for allocated and non-allocated observations.

Figure A.6: Share Who Misreport To Be a Job Stayer By Month of Non-employment

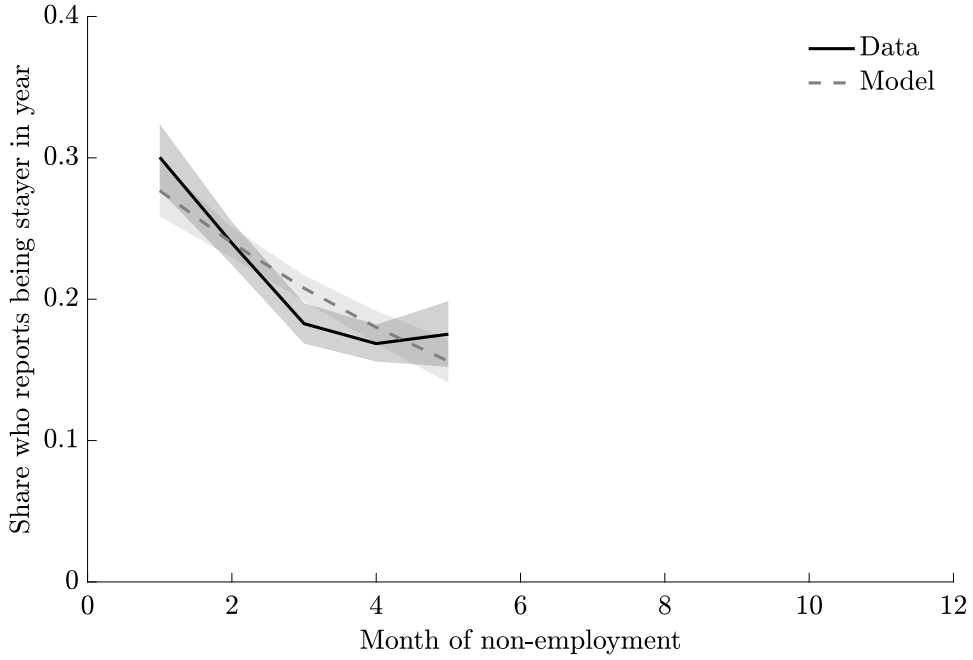

B Results Appendix

This appendix presents additional details and results from the partial equilibrium model.

B.1 Incorporating Age

To the extent that the measured EN rate also includes retirements, the methodology above continues to recover mobility rates by subgroup, except when comparing age groups. Even if all labor-market flow parameters are identical across ages, younger workers' wage distribution is mechanically shifted left because they have had less time to climb the job ladder. Correctly inferring mobility rates by age therefore requires an adjustment for time spent in the labor market.

Suppose workers enter the labor market nonemployed at age $a = 0$, and consider the population of workers with ages $a \in [0, \bar{A}]$. Assume the cross-sectional age distribution is uniform on $[0, \bar{A}]$ with density $1/\bar{A}$. Let $n(a)$ denote the nonemployment rate at age a, and let $E(a) \equiv 1 - n(a)$ denote the employment rate. Conditional on employment at age a, let $x(w, a)$ and $X(w, a)$ denote the wage density and CDF.

Nonemployment evolves as

$$n'(a) = -\,p\,n(a) \;+\; \delta\,\big(1 - n(a)\big), \tag{B.1}$$

subject to $n(0) = 1$. Solving yields

$$n(a) = \frac{\delta}{p+\delta} \;+\; \frac{p}{p+\delta}\,e^{-(p+\delta)a}, \qquad E(a) \;=\; \frac{p}{p+\delta}\big(1 - e^{-(p+\delta)a}\big), \tag{B.2}$$

and the average employment rate among workers with age at most $\bar{A}$ is

$$\bar{E} = \frac{1}{\bar{A}}\int_0^{\bar{A}} E(a)\,da = \frac{p}{p+\delta}\left(1 - \frac{1 - e^{-(p+\delta)\bar{A}}}{(p+\delta)\bar{A}}\right). \tag{B.3}$$

Fix w in the support of F and define

$$Y(w, a) \;\equiv\; E(a)\,X(w, a),$$

the mass of age-a workers who are employed at wages $\leq w$. $Y(w, a)$ satisfies

$$\frac{\partial}{\partial a}Y(w, a) = -\,s(w)\,Y(w, a) \;+\; F(w)\Big(p\,n(a) + \lambda^f E(a)\Big), \qquad Y(w, 0) = 0, \tag{B.4}$$

where

$$s(w) \;\equiv\; \delta + \lambda^f + \lambda^e\big(1 - F(w)\big).$$

Solving (B.4) by an integrating factor gives

$$Y(w,a) = F(w)\, e^{-s(w)a} \int_0^a e^{s(w)t} \Big(p\, n(t) + \lambda^f E(t) \Big)\, dt. \tag{B.5}$$

Using (B.2), the term in parentheses is affine in $e^{-(p+\delta)t}$:

$$p\, n(t) + \lambda^f E(t) = \underbrace{\frac{p(\delta + \lambda^f)}{p+\delta}}_{\alpha} + \underbrace{\frac{p(p - \lambda^f)}{p+\delta}}_{\beta} e^{-(p+\delta)t}.$$

Substituting into (B.5) and evaluating the integrals yields

$$Y(w,a) = F(w) \left[\frac{\alpha}{s(w)} \big(1 - e^{-s(w)a}\big) + \frac{\beta}{s(w) - (p+\delta)} \big(e^{-(p+\delta)a} - e^{-s(w)a} \big) \right], \tag{B.6}$$

with the understanding that if $s(w) = p + \delta$ the second term is interpreted by continuity (its limit).

The cross-sectional CDF among employed workers with age at most $\bar{A}$ is the employment-weighted average across ages:

$$G(w) \equiv \frac{1}{\int_0^{\bar{A}} E(a)\, da} \int_0^{\bar{A}} E(a)\, X(w,a)\, da = \frac{\int_0^{\bar{A}} Y(w,a)\, da}{\int_0^{\bar{A}} E(a)\, da}. \tag{B.7}$$

Define

$$I(z) \;\equiv\; \int_0^{\bar{A}} e^{-za}\, da \;=\; \frac{1 - e^{-z\bar{A}}}{z}, \qquad z > 0.$$

Then

$$\int_0^{\bar{A}} E(a)\, da = \frac{p}{p+\delta} \Big(\bar{A} - I(p+\delta) \Big), \tag{B.8}$$

and integrating (B.6) over $a \in [0, \bar{A}]$ gives

$$G(w) = \frac{F(w)}{\bar{A} - I(p+\delta)} \left[\frac{\delta + \lambda^f}{s(w)} \Big(\bar{A} - I\big(s(w)\big) \Big) + \frac{p - \lambda^f}{s(w) - (p+\delta)} \Big(I(p+\delta) - I\big(s(w)\big) \Big) \right]. \tag{B.9}$$

Equation (B.9) can be rewritten as

$$G(w) = \frac{F(w)}{1 + \kappa\big(1 - F(w)\big)} \big(1 + C(w; \bar{A}) \big), \tag{B.10}$$

where $\kappa \equiv \lambda^e/(\delta+\lambda^f)$ and

$$C(w;\bar{A}) \;=\; \frac{\lambda^e\big(1-F(w)\big)\,(p+\delta)}{(\delta+\lambda^f)\,\big(\lambda^f-p+\lambda^e(1-F(w))\big)} \cdot \frac{\dfrac{1-e^{-(p+\delta)\bar{A}}}{p+\delta} - \dfrac{1-e^{-\left(\delta+\lambda^f+\lambda^e(1-F(w))\right)\bar{A}}}{\delta+\lambda^f+\lambda^e(1-F(w))}}{\bar{A}-\dfrac{1-e^{-(p+\delta)\bar{A}}}{p+\delta}} \tag{B.11}$$

Fix w and define

$$z_0 \equiv p+\delta, \qquad z_1 \equiv \delta+\lambda^f+\lambda^e\big(1-F(w)\big), \qquad z_0>0,\; z_1>0.$$

Let

$$N(\bar{A}) \equiv \frac{1-e^{-z_0\bar{A}}}{z_0} - \frac{1-e^{-z_1\bar{A}}}{z_1}, \qquad D(\bar{A}) \equiv \bar{A} - \frac{1-e^{-z_0\bar{A}}}{z_0}.$$

The fraction in (B.11) is $N(\bar{A})/D(\bar{A})$.

For any $z>0$ and $\bar{A}\geq 0$,

$$0 \leq 1-e^{-z\bar{A}} \leq 1 \quad\Rightarrow\quad 0 \leq \frac{1-e^{-z\bar{A}}}{z} \leq \frac{1}{z}.$$

Hence

$$|N(\bar{A})| \leq \frac{1}{z_0}+\frac{1}{z_1}.$$

Using the same bound,

$$D(\bar{A}) = \bar{A} - \frac{1-e^{-z_0\bar{A}}}{z_0} \geq \bar{A} - \frac{1}{z_0}.$$

Therefore $D(\bar{A})\to\infty$ and grows linearly in $\bar{A}$.

Combining the bounds,

$$\left|\frac{N(\bar{A})}{D(\bar{A})}\right| \leq \frac{\frac{1}{z_0}+\frac{1}{z_1}}{\bar{A}-\frac{1}{z_0}} \;\xrightarrow[\bar{A}\to\infty]{}\; 0.$$

Thus, for fixed w, the bracketed fraction in (B.11) converges to zero (indeed at rate $1/\bar{A}$).

Away from the knife-edge $\lambda^f-p+\lambda^e(1-F(w))=0$, the prefactor in (B.11) is finite and does not depend on $\bar{A}$, so $C(w;\bar{A})\to 0$ as $\bar{A}\to\infty$. Hence, the convergence is $C(w;\bar{A})=O(1/\bar{A})$.

When $\lambda^f-p+\lambda^e(1-F(w))=0$ (equivalently $z_1=z_0$), the expression (B.11) has a removable singularity. Taking the continuous limit yields

$$C(w;\bar{A}) \;=\; \frac{\lambda^e\big(1-F(w)\big)}{\delta+\lambda^f} \cdot \frac{1-e^{-(p+\delta)\bar{A}}\big(1+(p+\delta)\bar{A}\big)}{(p+\delta)\bar{A}-1+e^{-(p+\delta)\bar{A}}}. \tag{B.12}$$

Since $e^{-(p+\delta)\bar{A}}\to 0$ and the denominator in (B.11) grows like $(p+\delta)\bar{A}$, it follows that $C(w;\bar{A})\to 0$

as $\bar{A} \to \infty$ in the knife-edge case as well (indeed $C(w; \bar{A}) = O(1/\bar{A})$).

B.2 Extended Model Targets

Table B.7 summarizes the full set of moments that we target in the extended model, as well as the particular parameter that each moment especially informs. The annual NE rate identifies p. The annual EN rate (overall and by initial wage), the distribution of nonemployment months in the eight-month BMS panel, and the joint panel distribution of employment states identify heterogeneity in flows $(\delta^1, \delta^2, \pi)$. The wage distribution—weighted twice—is the primary source of variation for κ; we supplement it with the distribution of annual wage changes and the joint distribution of wages 12 months apart for both all workers and job stayers. Conditional on κ, the share of job stayers (overall and by initial wage) distinguishes directed from undirected job-to-job mobility, λ^e versus λ^f.[24] Figure 6 illustrates several key targeted moments and the corresponding model fit.

Wage dynamics on the job are disciplined primarily by job-stayer moments: the distribution of year-on-year wage changes and the autocorrelation/joint distribution of wages 12 months apart identify $(\mu, \theta, \sigma, \zeta)$.[25] Job-loser moments—including wage changes around displacement and the relationship between wages before and after job loss (Figure 4b)—identify the heterogeneity parameter ω. Finally, responses about stayer status among BMS nonemployed workers discipline imperfect recall ν and the misclassification/recall parameter ε, together with the full joint distribution of employment status over the eight-month BMS panel. We target 14,427 moments for 12 parameters, so the model is overidentified.

Figure B.7 plots the observed and inferred true offer distributions as well as the resulting wage distribution in the data and extended model by each decade. The extended model further improves on the stylized model's ability to fit the observed wage distribution.

Figure B.8 plots the joint distribution of all workers and job stayers over wages at time t and $t + 12$ in the data and model. In both the data and model, a job stayer is someone who remained with the same employer during the previous calendar year.

Table B.8 shows the parameter estimates pooling all years of data.

[24] In the CPS, stayer status refers to calendar year t, while the "initial" wage is observed between December of $t - 1$ and June of t. We replicate this timing in the model.

[25] Because CPS wages are observed between December and June, wage changes for job stayers are measured with a timing mismatch that we replicate in the model.

Table B.7: Identification: Parameters and Targeted Moments (Extended Model, Pooled)

Parameter	Description	Value	Targeted moment	Data	Model
p	JFR of non-employed	0.019	NE rate	0.196	0.199
		(0.000)		(0.000)	(0.002)
λ^f	Undirected outside offers	0.015	Stayer share	0.756	0.754
		(0.001)		(0.001)	(0.001)
			Stayers by wage	See Figure 6b	
κ	Net upward mobility	0.967	Wage distribution	See Figure 6c	
		(0.090)			
			Wage change distribution, all workers	See Figure 6d	
			Distr. of wage changes of job losers	See Figure 6d	
			Mean wage change of job losers	-0.018	-0.023
				(0.003)	(0.002)
			Joint distribution over ORG 4–16	See Figure B.8	
δ^1	Separation rate (low-type)	0.012	EN rate	0.078	0.076
		(0.001)		(0.000)	(0.000)
δ^2	Separation rate (high-type)	0.004	EN by wage	See Figure 6a	
		(0.000)			
π	Share of high-type	0.442	Distr. over non-employment	See Figure 4a	
		(0.032)			
			Distr. over 8-month BMS		
μ	Long-run mean	0.004	Distr. of wage changes of stayers	See Figure 6d	
		(0.013)			
σ	Frequency of wage changes	0.122	St.d. of wage change of stayers	0.337	0.343
		(0.009)		(0.001)	(0.003)
ζ	Tail index of wage changes	1.568	Distr. of wage changes of stayers	See Figure 6d	
		(0.052)			
			Joint distribution over ORG 4–16, stayers	See Figure B.8	
θ	Autocorrelation of wages	0.036	Autocorrelation of wages of stayers	0.601	0.630
		(0.001)		(0.002)	(0.004)
ω	Mean offer difference	0.283	$\text{corr}(w_t, w_{t+12})$ of job losers	0.429	0.427
		(0.009)		(0.006)	(0.006)
			Mean wage of job losers by previous wage	See Figure 4b	
			Joint distribution over ORG 4–16, job losers		
ϵ	Recall/misclassification	0.003	Share unemployed who are stayers	0.229	0.262
		(0.000)		(0.008)	(0.007)

Figure B.7: Wage and Offer Distributions by Decade, Extended Model

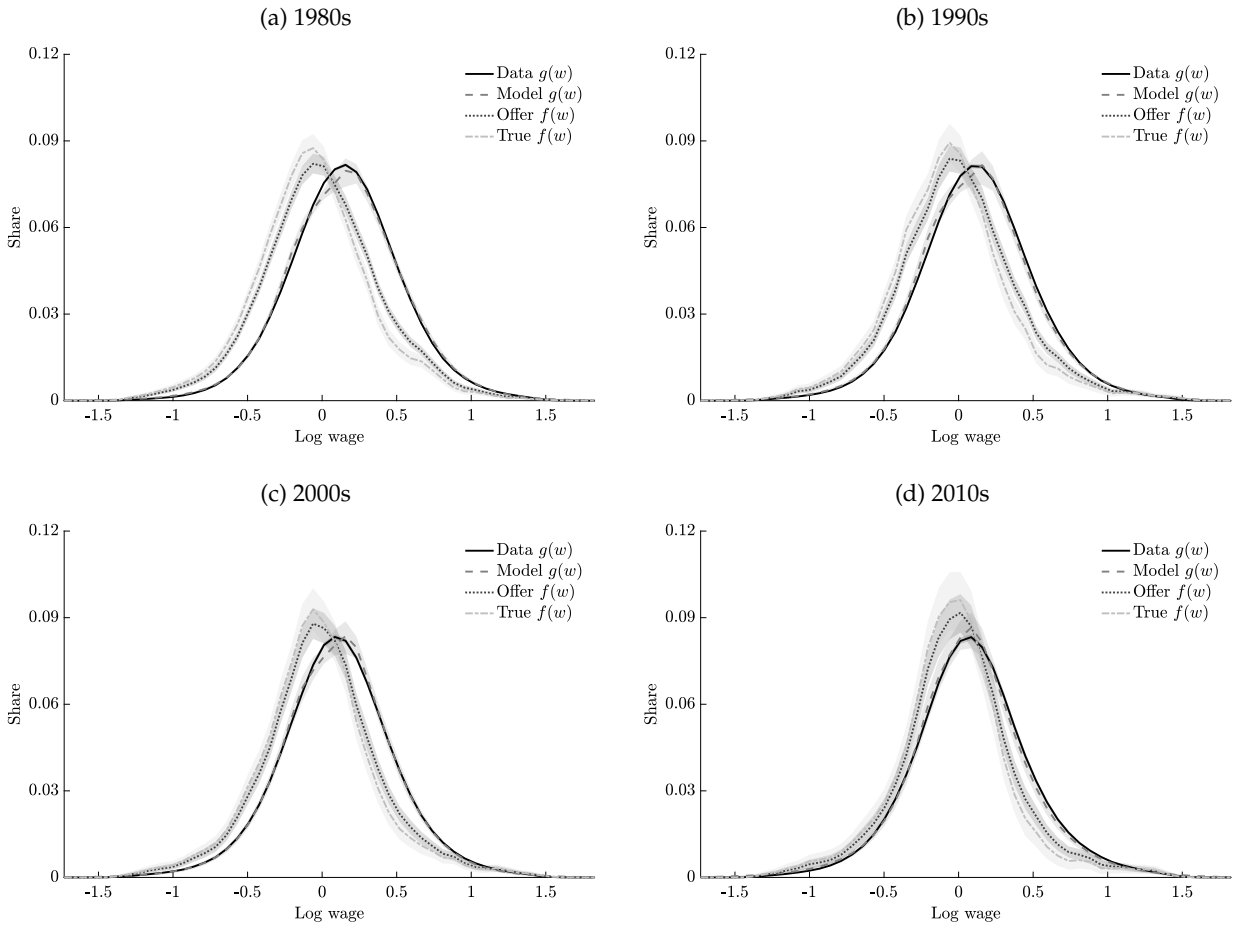

Notes: Each panel plots the distribution of wages of hires from nonemployment, the implied true offer distribution after adjusting for employment-status misclassification/recall unemployment, and the wage distribution among employed workers in the data and in the model, for the indicated decade. The sample restrictions and residualization procedure follow the notes to Table 4. *Source:* CPS ORG and ASEC 1982–2021.

Table B.8: Parameter Estimates Pooling All Years of Data in Extended Model

p	δ^1	δ^2	π	κ	λ^f	μ	θ	σ	ζ	ω	ϵ
0.019	0.013	0.004	0.434	0.958	0.015	-0.000	0.036	0.138	1.605	0.282	0.003
(0.000)	(0.001)	(0.000)	(0.034)	(0.090)	(0.001)	(0.014)	(0.001)	(0.012)	(0.066)	(0.009)	(0.000)

Figure B.8: Joint Distribution of All Workers and Job Stayers over Wages at t and $t+12$, Data and Model

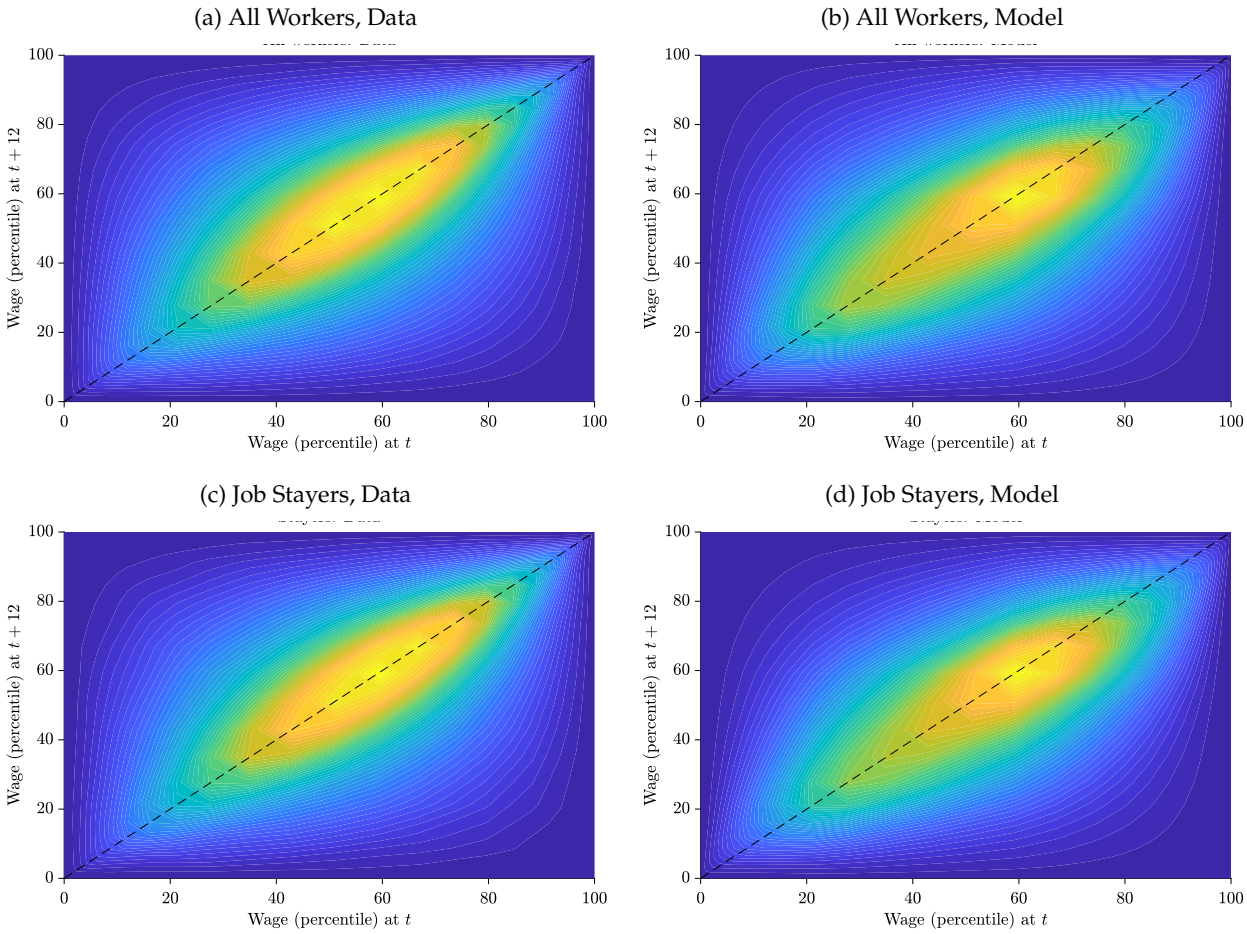

Notes: Each panel plots the joint distribution of workers over wages in month t and $t+12$. Job stayers are those who remain with the same employer in the previous calendar year, in both the data and model. The sample restrictions and residualization procedure follow the notes to Table 4. *Source:* CPS ORG and ASEC 1982–2021, and authors' calculations.

C Causes Appendix

This appendix contains details on the general equilibrium model.

C.1 Adding an Active Reservation Threshold

This subsection extends the model by allowing nonemployed workers to reject low offers. Let nonemployed workers receive offers at rate $\widehat{p}$ from an *untruncated* offer distribution $\widehat{F}(w)$ with density $\widehat{f}(w)$. Workers accept offers if $w \geq r$, where r is an *active reservation wage*. The effective job-finding rate is

$$p \equiv \widehat{p}\big(1 - \widehat{F}(r)\big).$$

Define the distribution of *acceptable* offers (i.e., the offer distribution conditional on $w \geq r$) by

$$F(w) \;\equiv\; \Pr\big(w' \leq w \,\big|\, w' \geq r\big) \;=\; \frac{\widehat{F}(w) - \widehat{F}(r)}{1 - \widehat{F}(r)}, \qquad w \geq r, \tag{C.13}$$

with density

$$f(w) \;\equiv\; \frac{\widehat{f}(w)}{1 - \widehat{F}(r)}, \qquad w \geq r. \tag{C.14}$$

Equivalently, for all $w \geq r$,

$$1 - \widehat{F}(w) \;=\; \big(1 - \widehat{F}(r)\big)\,\big(1 - F(w)\big), \qquad \widehat{f}(w) \;=\; \big(1 - \widehat{F}(r)\big)\,f(w). \tag{C.15}$$

Let $\widehat{\delta}$ denote the arrival rate of separations from employment to nonemployment. While employed, a worker receives *directed* outside offers at rate $\widehat{\lambda}^e$ and *undirected* outside offers at rate $\widehat{\lambda}^f$. If an undirected outside offer pays less than the reservation wage, the worker becomes nonemployed. Define the arrival rates of outside offers above the reservation wage as

$$\lambda^e \equiv \widehat{\lambda}^e\big(1 - \widehat{F}(r)\big), \qquad \lambda^f \equiv \widehat{\lambda}^f\big(1 - \widehat{F}(r)\big),$$

and define the effective separation rate to nonemployment as

$$\delta \;=\; \widehat{\delta} \,+\, \widehat{\lambda}^f\,\widehat{F}(r), \tag{C.16}$$

Let n denote the steady-state nonemployment rate and $E \equiv 1 - n$ employment. Steady-state flow balance implies

$$p\,n = \delta\,E.$$

Flow balance for the mass of employed workers at wage $w > r$ yields the Kolmogorov forward

equation

$$0 \;=\; -\Big(\delta + \lambda^f + \lambda^e\big[1 - F(w)\big]\Big)\, g(w) \;+\; f(w)\,\big(\delta + \lambda^f\big) \;+\; f(w)\,\lambda^e\, G(w). \tag{C.17}$$

or alternatively the first-order ODE

$$\Big(1 + \kappa\big[1 - F(w)\big]\Big)\, g(w) \;=\; f(w)\,\Big(1 + \kappa\, G(w)\Big), \qquad w > r, \tag{C.18}$$

with boundary condition $G(r) = 0$ and $F(r) = 0$. Solving yields the familiar Burdett–Mortensen mapping, now written in terms of the truncated offer distribution:

$$G(w) \;=\; \frac{F(w)}{1 + \kappa\big(1 - F(w)\big)}, \qquad w \geq r, \tag{C.19}$$

and the associated density

$$g(w) \;=\; \frac{(1+\kappa)\, f(w)}{\Big(1 + \kappa\big(1 - F(w)\big)\Big)^2}, \qquad w \geq r. \tag{C.20}$$

Thus, after redefining $(p, \delta, \lambda^e, \lambda^f, F)$ as the *effective* objects corresponding to acceptable offers, the equilibrium relationships between offers and wages take the same form as in the baseline model in which all offers are accepted. The only change is that our empirical methodology delivers estimates of the reduced-form objects $(\delta, p, \lambda^f, \lambda^e)$, not the true underlying objects $(\widehat{\delta}, \widehat{p}, \widehat{\lambda}^f, \widehat{\lambda}^e)$.

D Consequences Appendix

This appendix contains additional details on the wage-posting model.

D.1 Additional Cross-State Outcomes

While higher wages in high-κ states partly reflect higher productivity—in both the model and data—Figure D.9 shows that the labor share is higher in high-κ states. The relationship is essentially unchanged if we first residualize the labor share with respect to 4-digit sector.

Figure D.9: Cross-State Differences In The Structure Of The Labor Market and the Labor Share

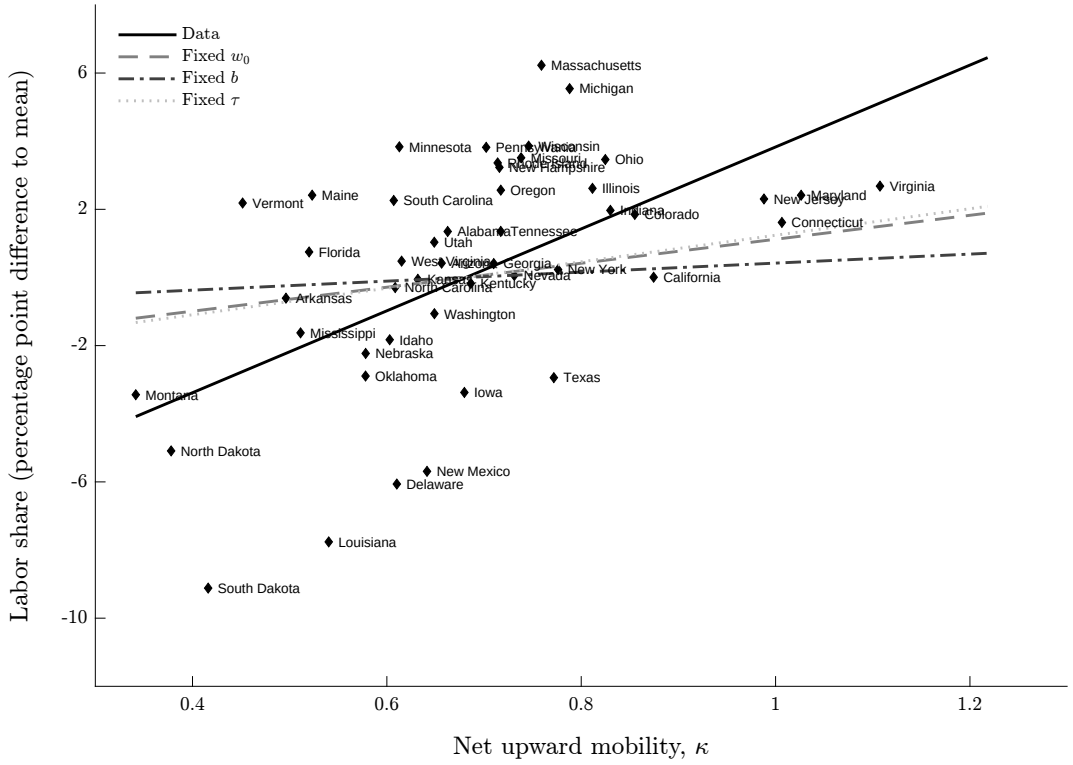

Notes: The unit of observation is a U.S. continental state. The labor share is compensation divided by value added at the state level. Fixed w_0 assumes a binding minimum wage. Fixed b assumes a binding reservation wage with a fixed flow value of nonemployment. Fixed τ assumes a binding reservation wage with a fixed replacement rate. *Source:* BEA, CPS BMS and ORG 1982–2021, and authors' calculations.

Figure D.10 plots the P1050 ratio of log offered wages in the data and model. As search efficiency in employment rises, the reservation wage tends to rise, compressing the offer distribution. This is particularly true with a fixed flow value of nonemployment, in which case the reservation wage response is the strongest. This evidence leads us to prefer the specification with a fixed replacement rate.

Figure D.11 plots the UI replacement rate. In the data, we construct this as the maximum weekly UI benefit over average weekly earnings in the state. In the model, it is the flow value

Figure D.10: Cross-State Differences In The Structure Of The Labor Market and the P1050 Log Ratio of Offered Wages

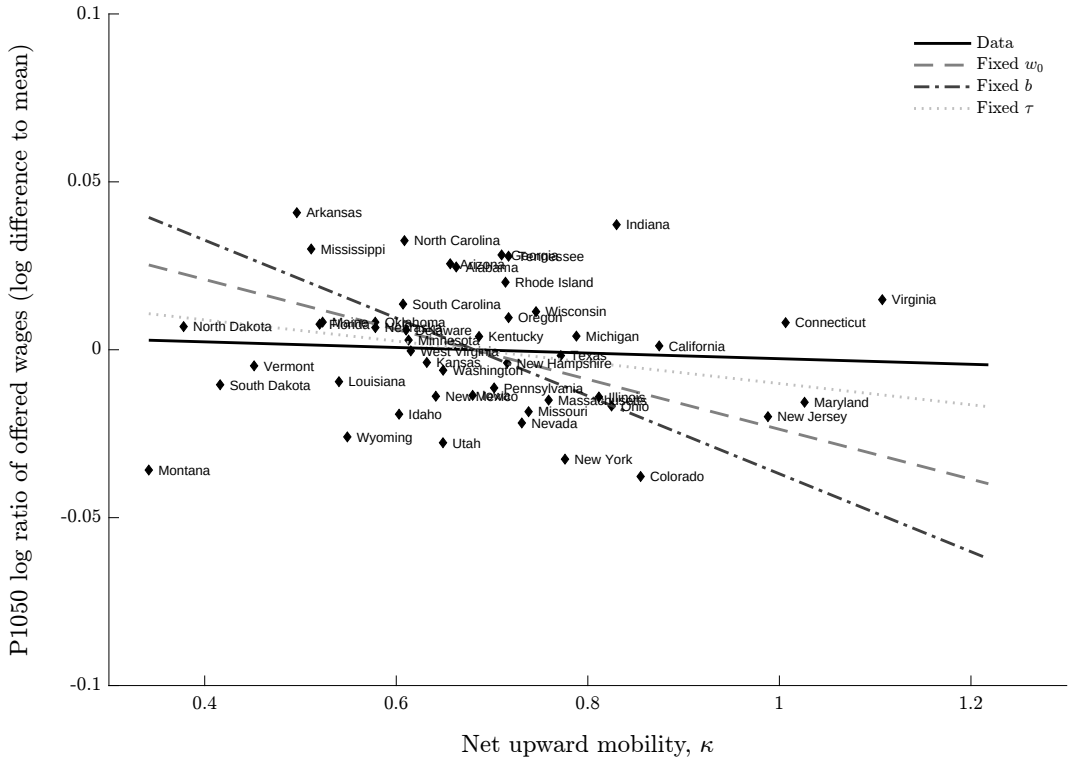

Notes: The figure plots the P1050 log ratio of offered wages. The unit of observation is a U.S. continental state. Wages are residuals that control for gender, race, education, and 3-digit occupation fully interacted with year, and are deflated by the average residual wage of an age-matched hire from nonemployment. Fixed w_0 assumes a binding minimum wage. Fixed b assumes a binding reservation wage with a fixed flow value of nonemployment. Fixed τ assumes a binding reservation wage with a fixed replacement rate. *Source:* BEA, CPS BMS and ORG 1982–2021, and authors' calculations.

of nonemployment b over the average earned wage. In both the data and the fixed w_0 and b specifications of the model, the UI replacement rate declines modestly with κ, as average earned wages rise with κ.

Figure D.12 shows that the relationship in Figure **??** does not result from the potentially confounding effect of a higher state minimum wage.

D.2 Cross-State Wages under Linear Utility

Figure D.13 plots the average offered and earned wage in the data and model against net upward mobility under linear utility. By construction, results are identical when the minimum wage is binding. With a fixed replacement rate, results are also similar under log and linear utility. The rise in earned wages with κ raises the flow value of nonemployment if it is determined as a fraction of average earned wages, which tampers the decline in the reservation wage resulting from a higher search efficiency in employment. With a fixed replacement rate, on the other hand, the results

Figure D.11: Cross-State Differences In The Structure Of The Labor Market and the UI Replacement Rate

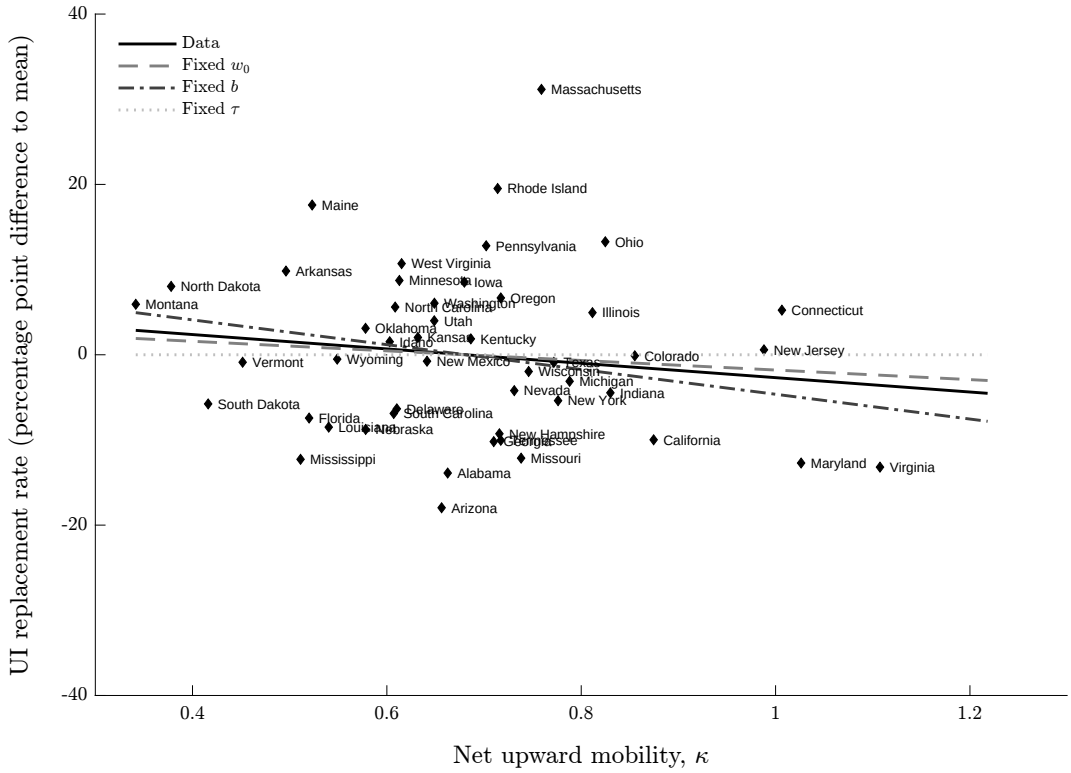

Notes: The figure plots the UI replacement rate. In the data, this is the maximum weekly benefit over average weekly earnings. In the model, it is b over average earned wages. The unit of observation is a U.S. continental state. Wages are residuals that control for gender, race, education, and 3-digit occupation fully interacted with year, and are deflated by the average residual wage of an age-matched hire from nonemployment. Fixed w_0 assumes a binding minimum wage. Fixed b assumes a binding reservation wage with a fixed flow value of nonemployment. Fixed τ assumes a binding reservation wage with a fixed replacement rate. *Source:* CPS BMS and ORG 1982–2021, U.S. Department of Labor, and authors' calculations.

under linear utility are substantially attenuated. The reason is that a higher search efficiency in employment results in a sharp fall in the reservation wage, offsetting much of the competition effect.

Figure D.12: Cross-State Differences In The Structure Of The Labor Market and the Minimum Wage

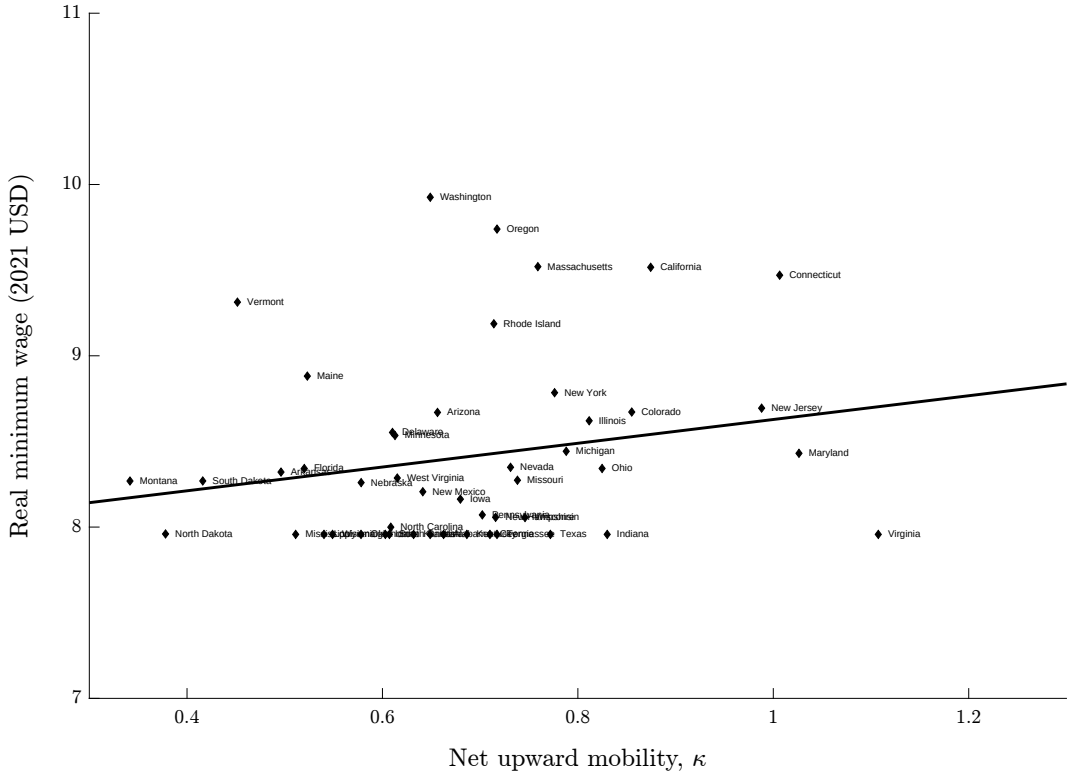

Notes: The unit of observation is a U.S. continental state. The minimum wage is the maximum of the state and federal minimum wage and the replacement rate is the maximum weekly replacement benefit over average weekly wages. Fixed w_0 assumes a binding minimum wage. Fixed b assumes a binding reservation wage with a fixed flow value of nonemployment. Fixed τ assumes a binding reservation wage with a fixed replacement rate. *Source:* CPS BMS and ORG, U.S. Department of Labor, 1982–2021, and authors' calculations.

Figure D.13: Average Offered Residual Wage (Top) and Average Earned Wage (Bottom)

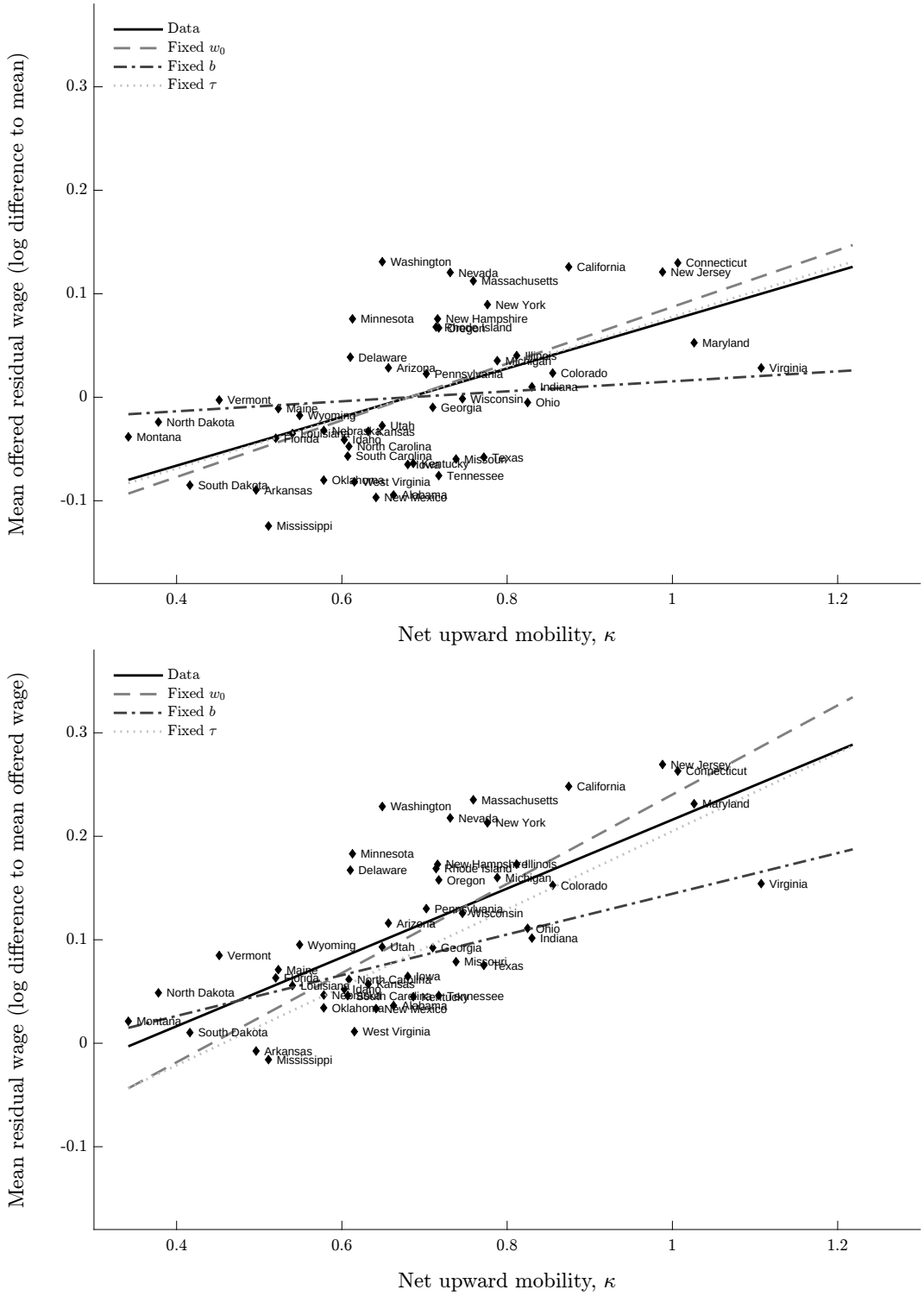

Notes: The unit of observation is a U.S. continental state. Wages are residuals that control for gender, race, education, and 3-digit occupation fully interacted with year, and are deflated by the average residual wage of an age-matched hire from nonemployment. Mean offered wages are expressed as deviations from their cross-state mean. Mean earned wages are expressed as deviations from the cross-state mean of *offered* wages. Fixed w_0 assumes a binding minimum wage. Fixed b assumes a binding reservation wage with a fixed flow value of nonemployment. Fixed τ assumes a binding reservation wage with a fixed replacement rate. *Source:* CPS BMS and ORG 1982–2021, and authors' calculations.

Figure D.14 plots the P1050 log ratio of offered wages in the data and model under linear utility. With linear utility, as the efficiency of employed search rises, workers become much less selective in what jobs they accept. The sharp fall in the reservation wage leads to a counterfactual, large increase in bottom tail inequality in offered wages. This is particularly true with a fixed flow value of nonemployment. For this reason, we prefer the log specification.

Figure D.14: Cross-State Differences In The Structure Of The Labor Market and the P1050 Log Ratio of Offered Wages, Linear Utility

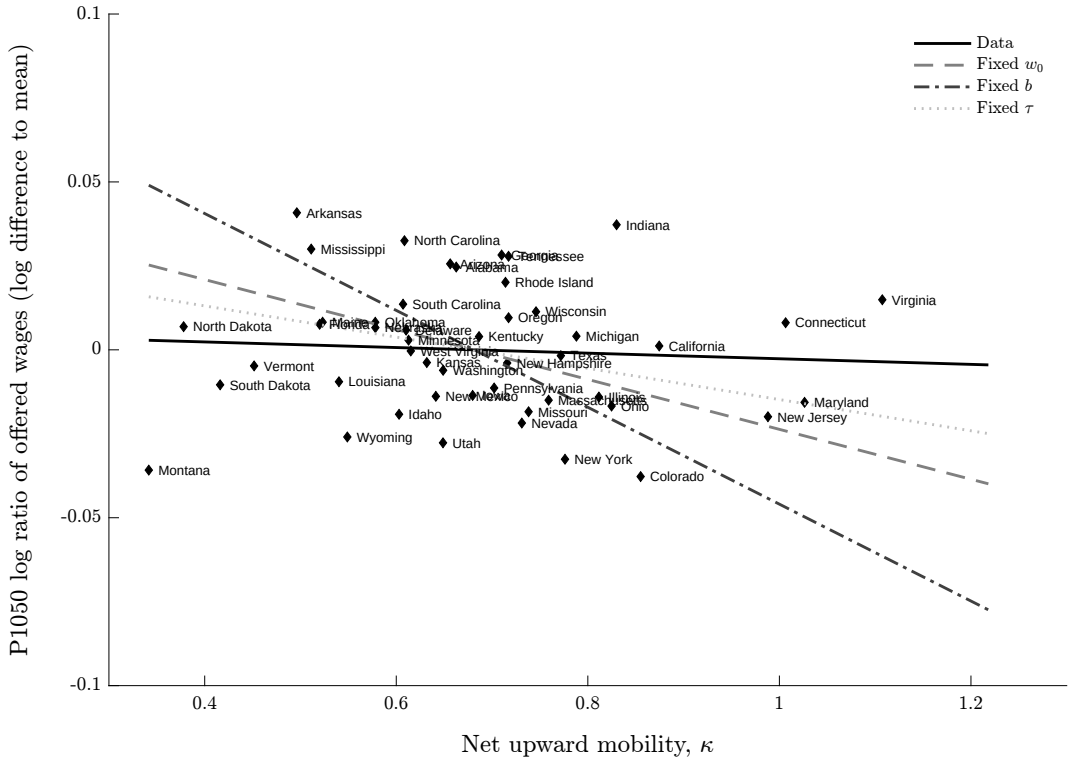

Notes: The figure plots the P1050 log ratio of offered wages. The unit of observation is a U.S. continental state. Wages are residuals that control for gender, race, education, and 3-digit occupation fully interacted with year, and are deflated by the average residual wage of an age-matched hire from nonemployment. Fixed w_0 assumes a binding minimum wage. Fixed b assumes a binding reservation wage with a fixed flow value of nonemployment. Fixed τ assumes a binding reservation wage with a fixed replacement rate. *Source:* BEA, CPS BMS and ORG 1982–2021, and authors' calculations.